FERMI
national accelerator laboratory

TM-667
1600.000

# OPERATIONAL TEST AND FIELD MEASUREMENT OF E5-1 MAGNET (I)

10 JUNE 1976

R. Yamada, H. Ishimoto, M. Price and R. E. Peters

ABSTRACT

The first E series dipole magnet with a long straight collared section and iron laminations was tested in a horizontal dewar by pool boiling method. The maximum field went up to 45.7 kG, which was confirmed by an NMR signal from lithium. The field quality at high field was found to be fairly good but at low field its behavior is very complicated due to the diamagnetism of superconductor.

## 1. INTRODUCTION:

Previously magnet number D-10-3 was tested extensively and reported.[1] To more deeply investigate the effects of construction errors, a 5 foot superconducting E series collared magnet (E5-1) was constructed and the field quality was measured very accurately. The wire which was used is unsoldered 23-strand cable made by IGC. For easy operation and interchangeability of coils, the coil was mounted in a simple horizontal cryostat. The test was done using the pool boilding method. The warm laminated steel core is made demountable and the whole magnet is mounted so that the dipole field is in a horizontal plane. The cross section of the magnet is shown in Fig. 1. The lamination size is a little smaller than that of the final design for the 22-foot Energy Doubler magnets. Its outside dimensions are 9.25 inches high and 15 inches wide with an inside circular hole of 7 inches diameter. The final design calls for laminations 10 inches higher, 15 inches

wide and with a 7.5 inch diameter. The end configuration of the magnet coils were not optimized, but we did get some useful information.

This magnet is the first collared E series one with a long straight section and iron laminations. It has a warm bore for field measurement. Of most interest was how high we could excite it. After many quenches, we eventually reached 45.7 kG. The absolute field value was confirmed using the NMR signals of proton and lithium samples.

After the ac loss measurement, the general field shape was measured with a Hall probe and the precise field measurements were done with a harmonic coil. The harmonic measurements were done in both dc and pulsed mode. In the dc mode, 4-, 6-, 8-, and 10-pole components were measured. For pulsed operation only 4- and 6-pole components were measured. They were all analyzed for normal and skew components. It was found that the normal 6-pole component changes drastically between pulsed and dc operation.

Also at low fields (0.5 kG~2 kG), which correspond to possible injection fields from the booster synchrotron, the field quality was investigated thoroughly. In this field region, the diamagnetism of the superconductor very seriously affects the field. Regardless of injection energy (0.5 kG~9 kG), it seems absolutely necessary to correct the normal 6-pole component.

2. TRAINING CURVE AND QUENCH BEHAVIOR:

In a previous test by the Energy Doubler Group this magnet went up to 5,000A without iron, corresponding to 40 kG. Therefore,

it was expected to hit well over 45 kG. As shown in Fig. 2, it started at about 40 kG and eventually reached 45.7 kG. The short sample data curve of the wire and load line of E5-1 are shown in Fig. 3. The solid load line corresponds to a bore field of 10.06 G/Amp at low field and shows a small saturation effect due to iron above 35 kG. The calculated value of the transfer function by S. Snowdon is 10.02. The dashed loaded line labeled "top edge field" corresponds to the calculated highest field at the innermost turn of the inner layer in the straight region of the coil. The total length of the core is 56 inches and the overall length of the coil is ~66.5 inches. It is expected that the highest field in the coil still occurs in the winding at the end. We have not measured how large the field is there, but it is estimated to be roughly a few percent higher than the dashed line.

The maximum current in the magnet was much smaller than the short sample limit. Even without iron the maximum current did not reach the short sample value. The wire used for this magnet was made by IGC. For some reason this wire (roll #72) was very unstable, and we got two short sample limit lines; one for a soldered cable and one for an unsoldered cable. The maximum field points lie between these two lines.

The ramp rate dependence of the maximum current is shown in Fig. 4. As was observed by the Energy Doubler Group for the case without core, it is flat up to at least 9 kG/sec.

The behavior during a quench was measured using the computer program "QUENCH". The current and the voltage across the magnet are shown in Fig. 5. The energies dumped into the magnet and a dump resistor were calculated on-line. Typically 12 kJ went into the magnet and 42 kJ went into the dump resistor of 50 mΩ during a quench of 4,500A at safety setting of 0.6V. The resistance of the magnet after quench is also calculated and shown in Fig. 6. It depends on the setting of the safety circuit (i.e., the energy spent in the coil), and typically is in the range of 10 to 30 mΩ. It shows that the propagation of the normal state stops about 170 msec after quench. A modified two channel "QUENCH" program for top and bottom coils was also applied and used to investigate which coil is quenching first.

## 3. EXCITATION CURVE MEASURED BY AN NMR CIRCUIT:

To get an absolute field value, NMR technique is the best. It requires a good field homogenity over the entire sample. With a proton sample, we need a very high frequency apparatus to measure up to 45 kG (192 MHz). We do not have such equipment now, and we have to use $^{7}$Li or D samples. They have smaller resonant frequency and hence the S/N ratio is worse than that of proton samples. Another important thing to avoid is saturation of the nuclear spin system due to the radio frequency. For this purpose, a small quantity of paramagnetic ions were mixed in the liquid sample.

The NMR circuit we used was designed and built by Dr. K. Bores at CERN for g-2 magnets, and it has a frequency range from 27 MHz

to 92 MHz. We used a small liquid sample (~0.1 cc) which was made of $LiClO_3$, $H_2O$ and $Cu(ClO_3)_2$. Even with this small sample, we could not observe a clear signal directly from $^7Li$ on the scope, and we applied signal averaging technique using a computer. The S/N ratio of $^7Li$ was very small partly because of the fluctuation of the power supply current.

The pictures of proton and lithium signals at 20, 30 and 44 kG are shown in Fig. 7. To take these pictures, the magnet was operated in the dc mode up to 44 kG without quenching. The transfer factor derived from this measurement is given in Fig. 8. It starts to decrease drastically at around 35 kG, and at 45 kG it is smaller than the low field value by o.5%. This fact should be attributed to the iron saturation. To support this, the magnetization curve, which is shown in Fig. 9, shows an upward swing above 35 kG. The downward drop between 10 and 35 kG indicates a slight deformation of the magnet resulting in a minor change in the inductance. The present steel laminations are smaller than those in the final design as mentioned before. The calculated saturation for the final design is 0.3% according to S. Snowdon.

The other remarkable thing is that the descending transfer factor is a little bit ($4 \times 10^{-4}$ at 20 kG) larger than the ascending one. This fact is mostly due to the remanent field coming from diamagnetism of the superconductor.

Fig. 7 also yields information about the homogeneity of the field. The line width of the liquid sample is almost determined by

the field homogeneity. For example, at 20 kG and at the best point, it is about 0.1G or so over the sample ($\lesssim$0.1 cc). These pictures were taken at the best point and do not represent all the points in the magnet. We scanned the longitudinal field shape with the NMR at 20 kG for gross checking. At the far end of the magnet, the variation of the field was $\pm 6 \times 10^{-4}$.

4. AC LOSS:

The dependence of the ac loss on maximum field is shown in Fig. 10. It does not show an abrupt break at around 30 kG as was observed in D-10-3.[1] This fact suggests that the collared magnet is mechanically more rigid than the banded one. But a closer look shows that the data above 30 kG may manifest some unstability, which may be due to a minute motion at the ends. In Fig. 10 calculated ac loss values of the coil from wire data are shown by x marks at 45 kG.

The losses corresponding to a starting field of 9 kG were also measured and shown in Fig. 10.

5. HALL PROBE MEASUREMENT:

Field measurements with a Hall probe (F. W. Bell HTT8) were done to get the general field shape and also to check the data of harmonic analysis. Fig. 11 shows the vertical field distribution along its axis at 4,000A. The effective magnetic end is about 2.80 inches outside the edge of the iron. It is the same within a few mils at 1,000A.

The remanent field distribution along the center line was measured during cool down and then after excitation up to 10, 20, 30 and 40 kG. The data are shown in Fig. 12. The contribution from the iron laminations is about 2.5G and has a small bump at the iron edge. The remanent fields after excitation are 10~12G and have prominent peaks at the coil end. This value is about twice that of D-10-3 (5~6G), which is made of the 17-strand cable. The E5-1 is wound with the 23-strand cable and should have a larger remanent field. The amplitude also depends on how the magnet was shut off, and in Fig. 12 the curve for 30 kG is lower than for 40 kG due to a change in the process of shutting off the power supply. Well inside the magnet the distribution has a periodic structure only after high field excitation (30 and 40 kG). The remanent field due to iron laminations has no such structure and this periodicity should be attributed to the superconducting coil itself. As we can see in the above, the remanent field strongly depends on the history of the magnet. After a quench, the remanent field strength was measured as a function of maximum excitation field. Fig. 13 shows the results. At around 2 kG, the value starts to decrease. As is well known, the remanent field is strongly connected with the magnetization loop of a superconductor.[2,3] The above value of 2 kG corresponds to what is called the saturation field, where the magnetic flux penetrates completely into the filaments. The penetration field of this wire is about 1.2~1.5 kG according to the hysteresis data of this wire. When the power supply was tripped off while going down,

the remanent field value became slightly smaller than usual. The main part of the remanent field is due to persistent current inside the superconducting filaments, which stays constant. There are coupling currents between filaments and another coupling current between strands. They make extra remanent fields which decay as shown in Fig. 14. These coupling currents decay due to resistance of matrix copper and to contact resistance between strands.

The remanent field was mapped both in the median and vertical planes as shown in Fig. 15 and 16. After excitation up to a high field, it had a large 6-pole component, which is about 20 times as large as that in the Main-Ring magnet. The remanent field, due to the iron laminations, has practically no higher order components. Even after a quench, the field distribution is somehow different than that of the normal state. This means that some trapped flux still exists inside the coil, because only part of the coil goes normal. The distribution in the vertical plane is not symmetrical. The physically bottom part has a large remanent field. This seems to arise from an asymmetrical trapped flux distribution between the top and bottom parts.

To have a rough idea of field shape at high current and for comparison with other measurements, the field distribution in the median plane was measured at 4,000A. The result is shown in Fig. 17. We can see a positive 4-pole field, but it is very difficult to get information of a 6-pole term with a Hall probe measurement.

To investigate the field shape at low field with and without the current reversal, the Transrex power supply was replaced with a small but more stable power supply in this current region. The field shape at low field is very sensitive to the history of the superconducting wire. After 40 kG excitation, it was measured at 0A (remanent field), 50A and 100A when ascending. The data are shown at the bottom of Figs. 18, 19, and 20. We can see that the 6-pole component disappears completely around 0.5 kG.

Again exciting up to 40 kG and coming down to zero current, the magnet was excited to -5 kG (which is more than twice the penetration field value). Then after measuring the remanent field shape, the magnet was again excited positively. The field was remeasured at 50A and 100A when ascending. The results are shown at the top of Figs. 18, 19, and 20. By reversing the field, the 6-pole coefficient was changed from positive to negative at the remanent field and at ascending 0.5 and 1 kG. More detailed and extensive measurements were done in the harmonic analysis and we will discuss them later.

## 6. HARMONIC ANALYSIS:

Various kinds of higher order harmonics (4-pole, 6-pole, 8-pole, and 10-pole) were measured (in dc and pulsed modes from low field to 40 kG) by using the CAMAC-PDP11 system.[1] In addition to that the harmonic components have carefully been measured under dc conditions at low field (remanent field, 0.5 kG, 1 kG and 2 kG) taking into account the history of excitation.

The field distribution on the median plane (y = 0) is given as

$$B_y(x) = B_0(1 + b_1x + b_2x^2 + b_3x^3 + b_4x^4 + \ldots)$$

$$B_x(x) = B_0( \quad a_1x + a_2x^2 + a_3x^3 + a_4x^4 + \ldots)$$

$B_0$ is the center field, $b_n$ and $a_n$ are respectively the normal and skew 2(n+1)-pole coefficients. The harmonic coil which was used is a Morgan type and has a 1.5 inch diameter and a 40 inch length. It was placed in the uniform region of the magnet, away from both ends and any effects they might cause.

6.1 Two Dimensional Region.

6.1.1 DC Measurement.

Various harmonic components in the dc mode were analyzed and the normal and the skew components are given in Figs. 21, 22, and 23, where field values are given at 0.75 inches. Also in these graphs, the virgin operation is shown with dotted lines. The corresponding coefficients are shown in Figs. 24, 25, and 26.

The 4-pole component was much improved compared with D-10-3. The normal component has a small hysteresis, which may be due to asymmetrical magnetization of wire. The fairly large normal and skew 4-pole component may be due to miscentering of the coil in the iron laminations or due to a deformed lamination core. It will be interesting to

see if this component will disappear after removing the iron.

The 6-pole component exhibits a very complicated behavior. The skew component has no hysteresis, which suggests that it arises mainly from a construction error and not from the magnetization effect. Misalignment of upper and lower coil shells and shifting of upper and lower keys are most probable causes.

The normal component shows a prominent hysteresis loop. Below 10 kG its behavior is very interesting. The small insert in Fig. 25 shows the behavior at low field (below 5 kG). The field shape after many excitations changes from concave to convex at ~500G when ascending and in an opposite way at 5.5 kG when descending. After exciting the magnet up to 40 kG and bringing it down to zero, if we reverse the field direction the field shapes behave quite differently as was described in Section 5. Typical reconstructed field shapes are shown in Figs. 18, 19, and 20. They reproduce the results of the Hall probe measurements very well.

As we can see by the similarity between this hysteresis loop and the magnetization curve of the superconductor, these effects come from the diamagnetism of the superconductor. We can not avoid this problem so long as we use superconductor. These effects could be decreased by decreasing the filament size.

As mentioned in the previous section, the iron laminations are a little bit saturated and their small effect on the normal 6-pole component can be seen above 30 kG. This small saturation effect is one of the advantages of warm iron.

The higher 8- and 10-pole components are shown in Figs. 23 and 26. The skew 8-pole component is quite high compared with the other components. The normal 10-pole component changes its sign at around 20 kG.

All these harmonic components for dc measurement are summarized in Table I.

6.1.2 Remanent Field.

As for the remanent field, we first got a rough idea from the Hall probe measurement as shown in Figs. 15 and 16. The more detailed measurements were done using the harmonic coil. Fig. 27 shows

2-, 4-, and 6-pole amplitudes as a function of the maximum excitation field for the virgin and subsequent excitation. Once we go higher than 2 kG or so, the saturation field, the value of remanence stays almost constant. The remarkable thing is that the remanent field includes a very high 6-pole component, compared with the 4-pole one, and these values change quite a lot after quenching. Their higher order coefficients are given in Fig. 28.

6.1.3 Pulsed Measurement.

The 4-pole and 6-pole components were measured in the pulsed mode to investigate the eddy current effect in the conductor itself and in the other metalic parts. While the field is ramped up and down, the harmonic coil is kept stationary and the data corresponding to predetermined fields are stored. It is then rotated by 1/32 of a rotation. This procedure is repeated at 32 different points on the circumference. The detailed explanation is given in a previous report.[1]

The results are shown in Figs. 29, 30, 31 and 32. The 4-pole amplitudes and coefficients

agree fairly well with those in the dc mode, so do the skew 6-pole components. However, the normal 6-pole components shifted as a whole and the hysteresis loop got fat (now the difference between up and down is ~5G at 20 kG instead of 3G for the dc mode). At low field, the behavior is quite different from that in the dc mode; therefore, it is absolutely necessary to do pulsed measurement on field shape, especially at low field, for the determination of correction coil.

6.2 End Effect.

To measure the contribution of the magnet ends to the harmonic component, the harmonic coil was positioned to cover the entire region of one end and the 4- and 6-pole components were measured. The coil is 3 feet long and the signal which was obtained comes partly from the 2-dimensional region. Using the data obtained in the 2-dimensional region, the integrated end field over 1 foot was estimated and is shown in Figs. 33 and 34. The 4-pole component is somewhat higher than at the center and distorted, as seen in the change of sign. The 6-pole component is drastically higher than at the center (~30 times). This result comes from misdesign of the end, and we should have a better configuration with the next E5-2 magnet.

REFERENCES:

[1]R.Yamada et al., Operational Test and Field Measurement of D-10-3, Fermilab Internal Report TM-651, March 26, 1976.

[2]W. B. Sampson et al., Magnetic Measurements of Superconducting Synchrotron Magnets, Proc. Int. Conf. on Magnet Technology, September 1972.

[3]M. A. Green, Residual Fields in Superconducting Magnets, Proc. Int. Conf. on Magnet Technology, September 1972.

[4]M. E. Price and R. Yamada, Hysteresis Loss Test of Superconducting Wires, Fermilab Internal Report TM-639, December 15, 1975.

TABLE I

Summary of the Harmonic Coefficient at the Ascending Field

| | | 5 kG | | 10 kG | | 20 kG | | 30 kG | | 40 kG | | |
|---|---|---|---|---|---|---|---|---|---|---|---|---|
| | | $b_n$ | $a_n$ | $b_n$ | $a_n$ | $b_n$ | $a_n$ | $b_n$ | $a_n$ | $b_n$ | $a_n$ | |
| Quad- | n=1 | 3.47 | 3.23 | 3.51 | 3.27 | 3.78 | 3.18 | 4.15 | 3.25 | 4.4 | 3.3 | x $10^{-4}$/cm |
| Sex- | 2 | -2.49 | -1.03 | -1.40 | -0.95 | -0.97 | -0.94 | -0.82 | -0.92 | -0.60 | -0.86 | x $10^{-4}$/$cm^2$ |
| Oct- | 3 | -1.1 | -9.0 | -1.7 | -9.2 | -2.5 | -7.7 | -3.2 | -6.8 | -3.8 | -6.2 | x $10^{-6}$/$cm^3$ |
| Dec- | 4 | 0.28 | -0.21 | 1.6 | -0.38 | 0.28 | -0.52 | -1.32 | -0.55 | | | x $10^{-6}$/$cm^4$ |

$$B_y\ (y=0) = B_0(1 + b_1x + b_2x^2 + b_3x^3 + b_4x^4 + \ldots.)$$

$$B_x\ (y=0) = B_0(\quad a_1x + a_2x^2 + a_3x^3 + a_4x^4 + \ldots.)$$

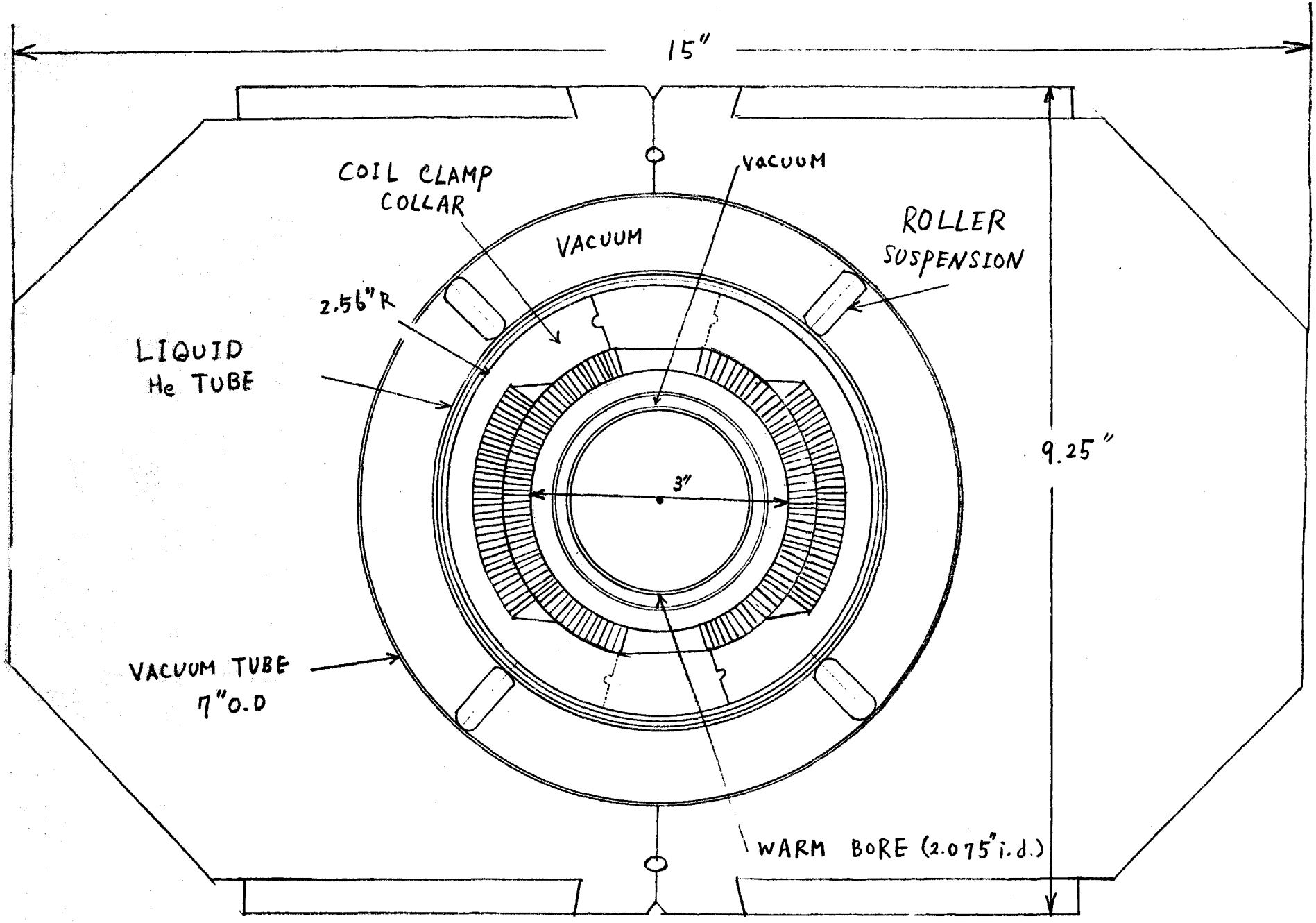


Fig. 1 Cross Section of E-5-1

May 13-14, 1976

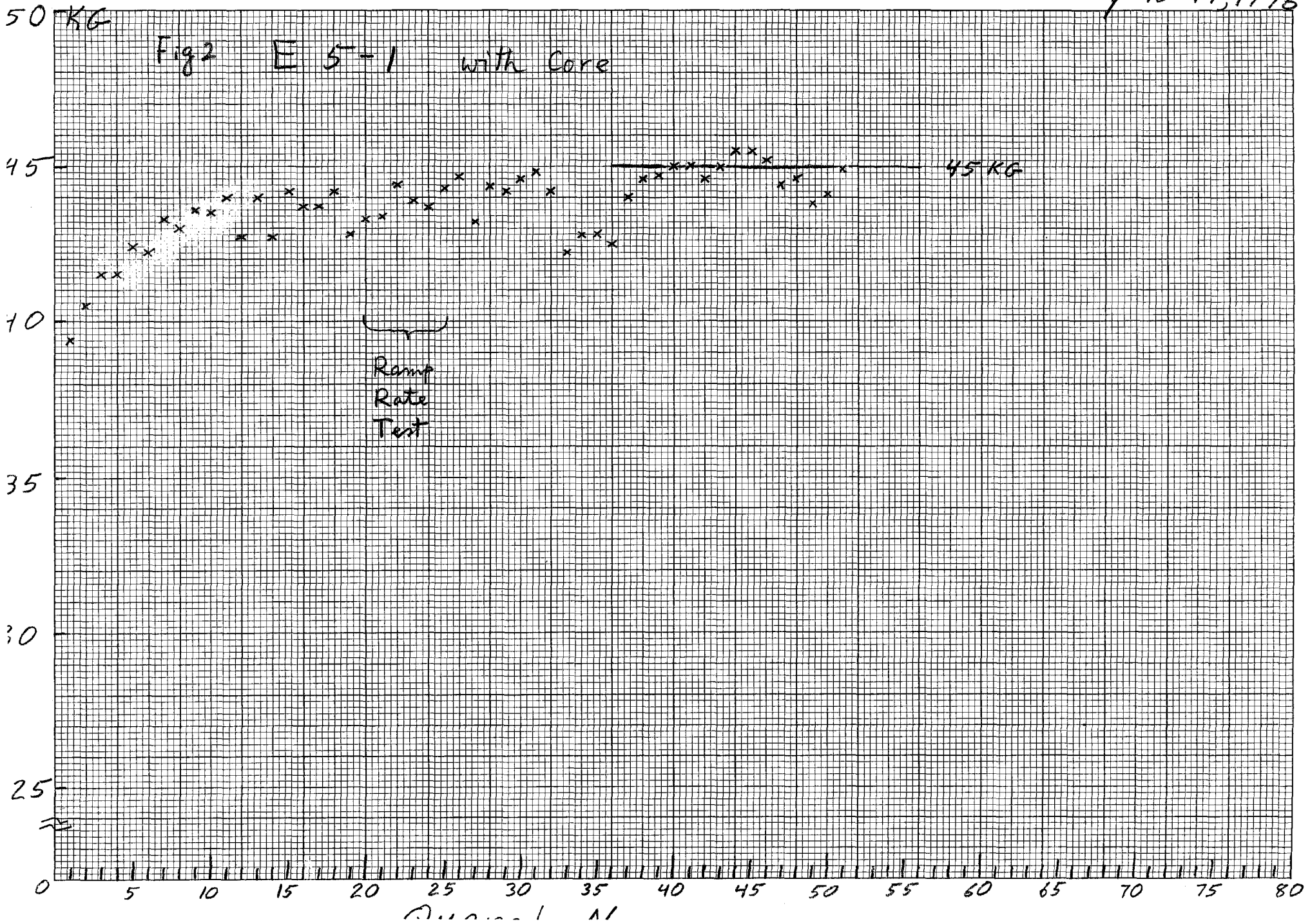


Fig 2 E 5-1 with Core

5/14/76

Fig. 3 Load line and Short Sample Data

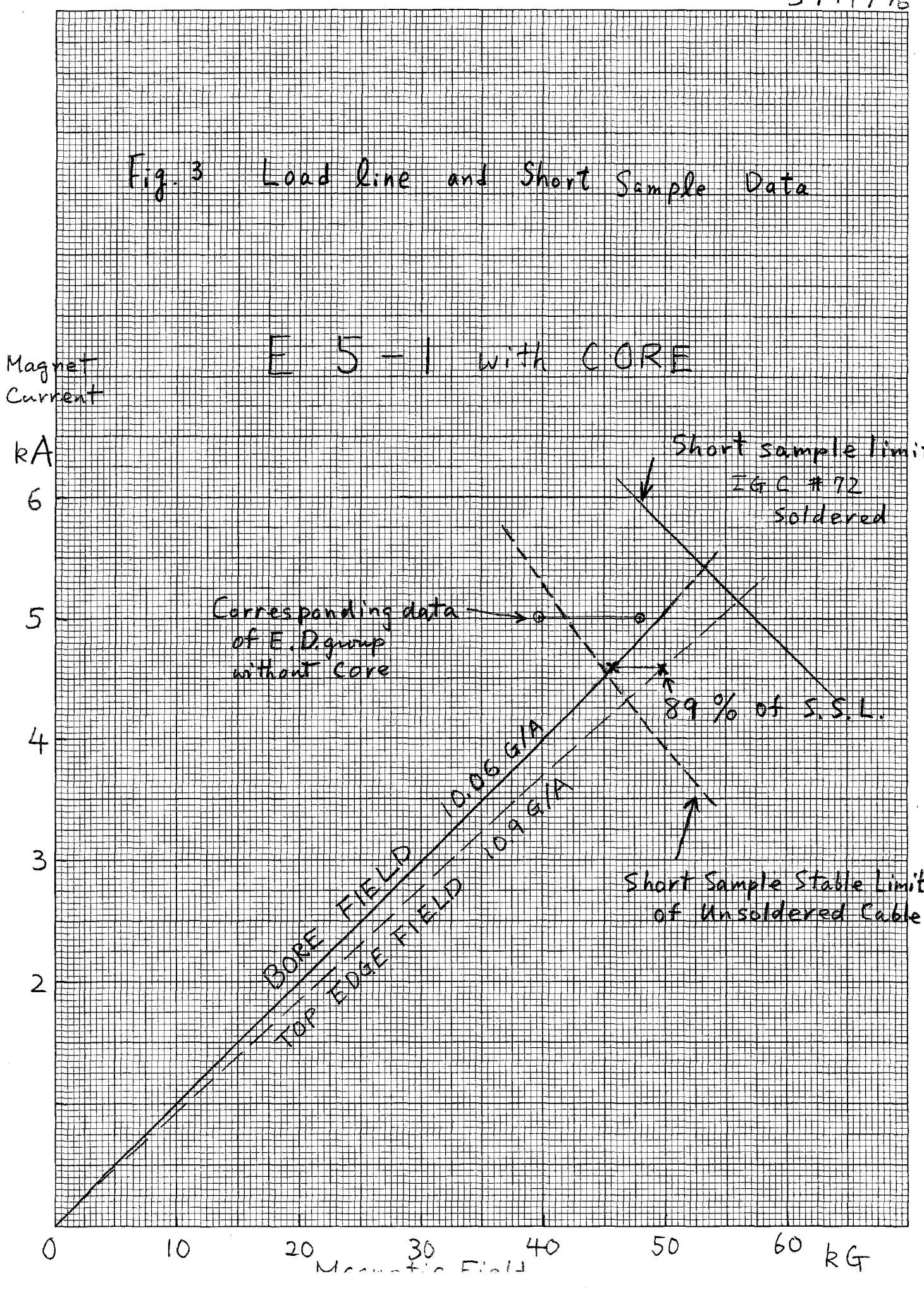

May 14, 1976

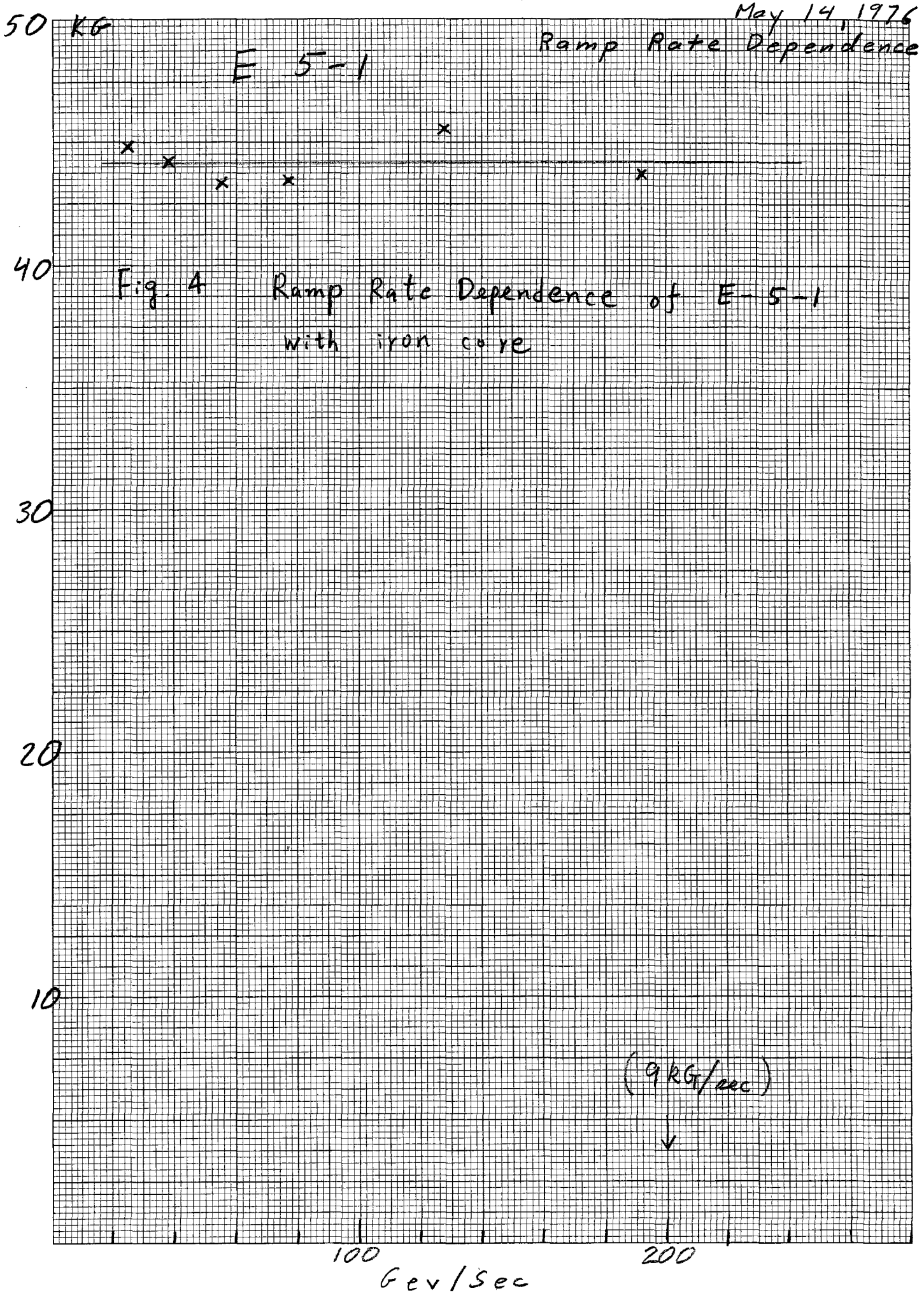


Fig. 4 Ramp Rate Dependence of E-5-1 with iron core

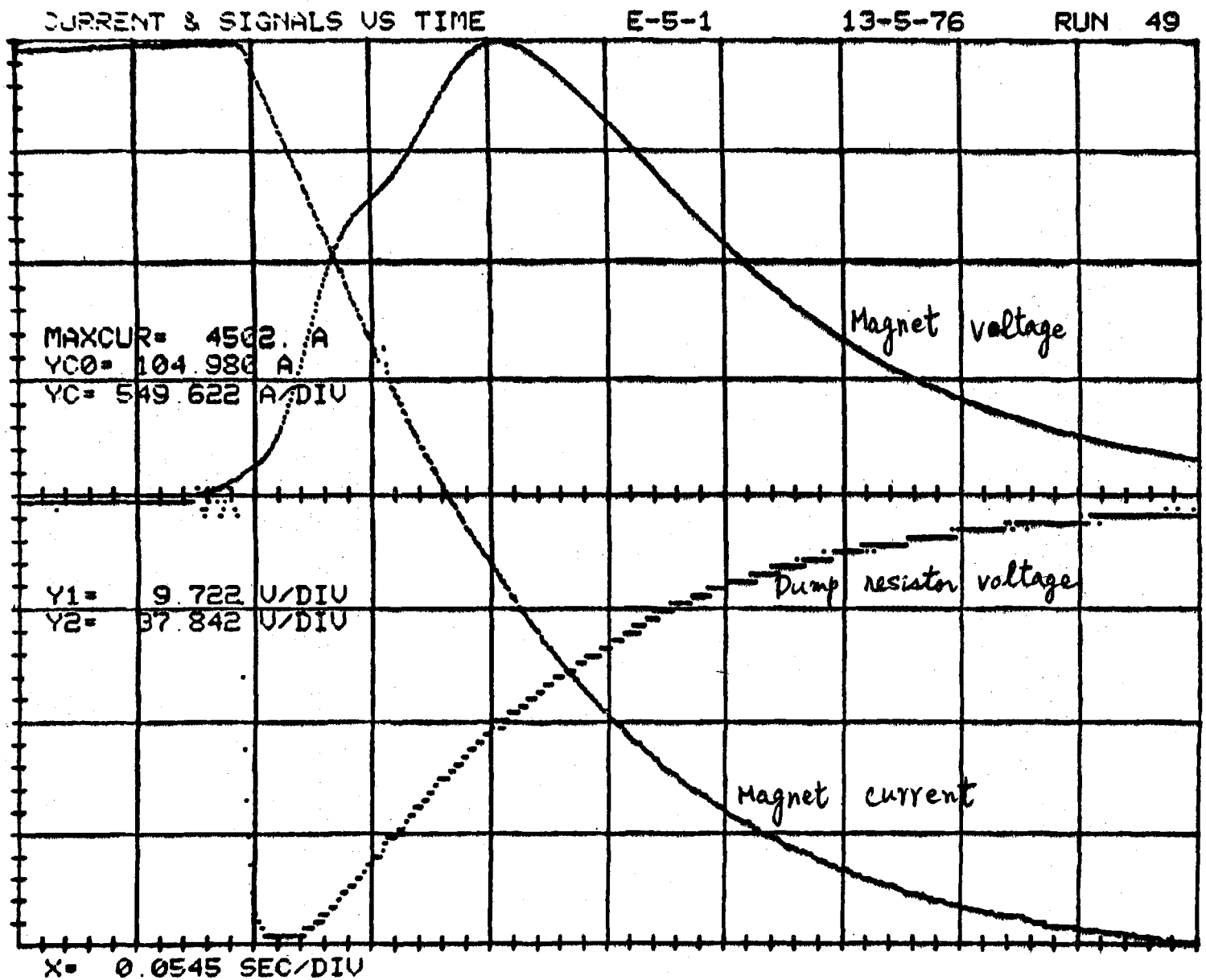


Fig. 5 Transient Behavior at Quench

Fig. 6 Resistance of Coil after Quench

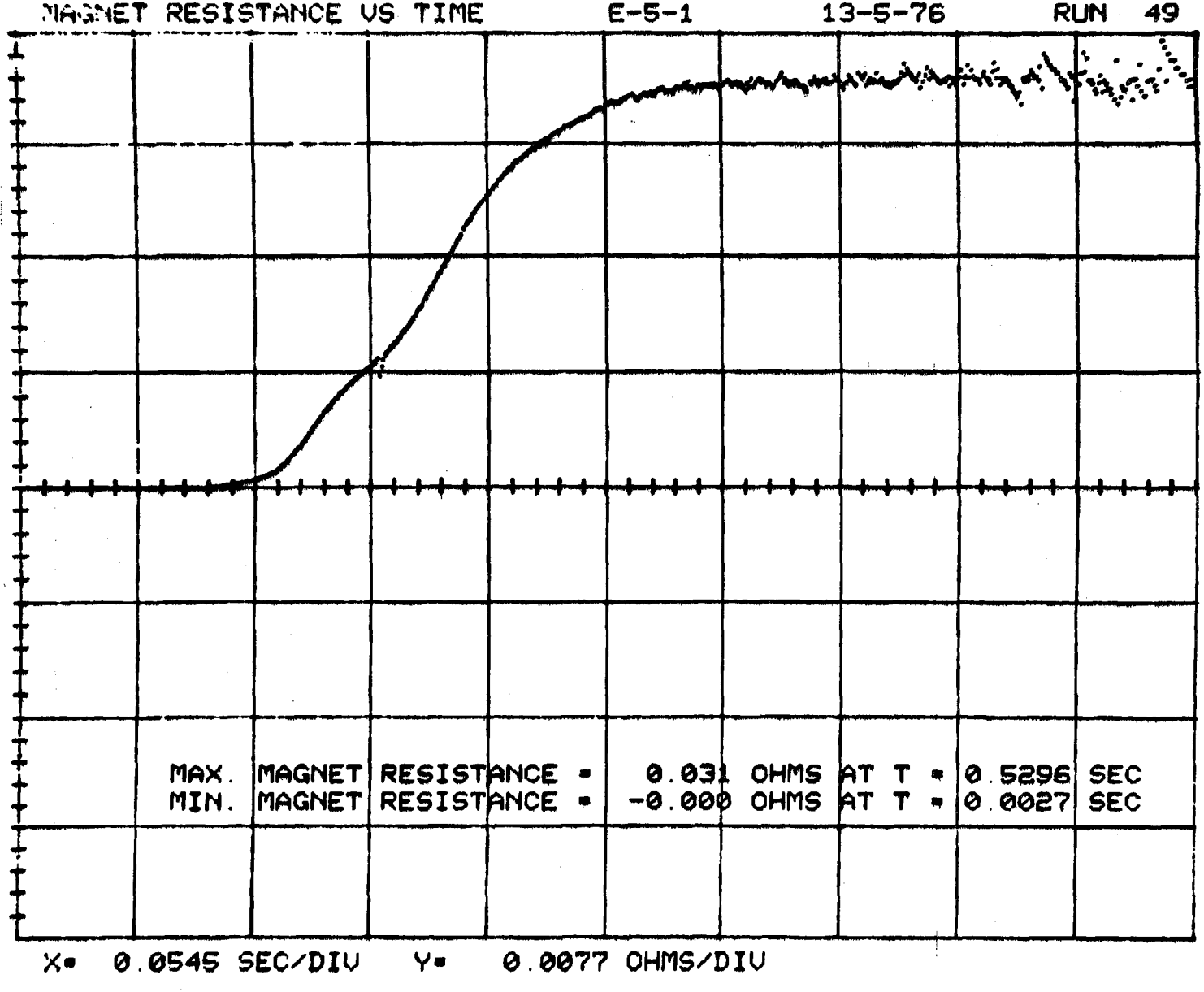

NMR SIGNAL IN THE E5-1

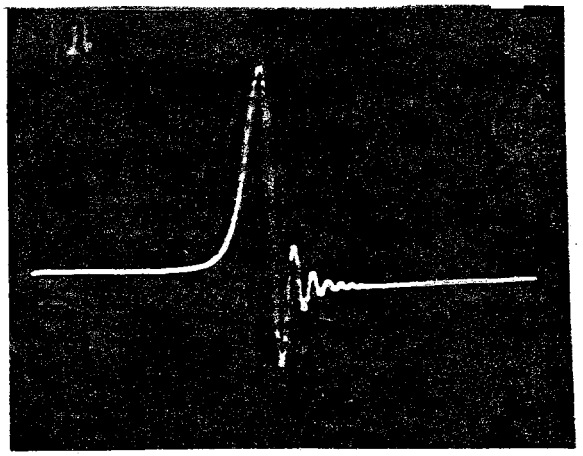

Proton

2,000A
85.661 MHz
= 20.12 kG

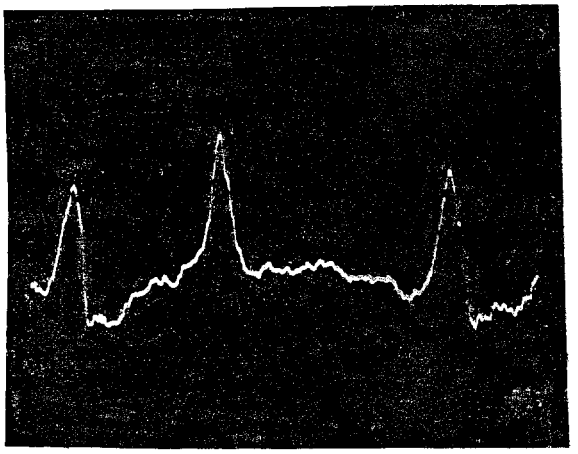

$^{7}Li$

3,000A
40.253 MHz
= 30.19 kG
after signal averaging

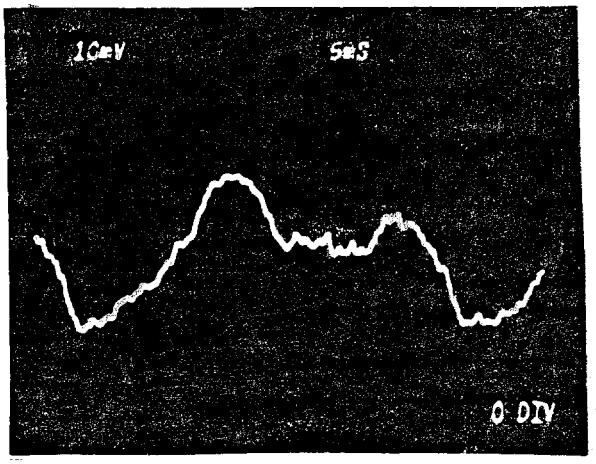


$^{7}Li$

4,400A
72.954 MHz
= 44.09 kG
after signal averaging

FIGURE 7

NMR SIGNAL FOR E5-1 MAGNET

5/28/76

E-5-1

Fig. 8 Transfer Function using NMR

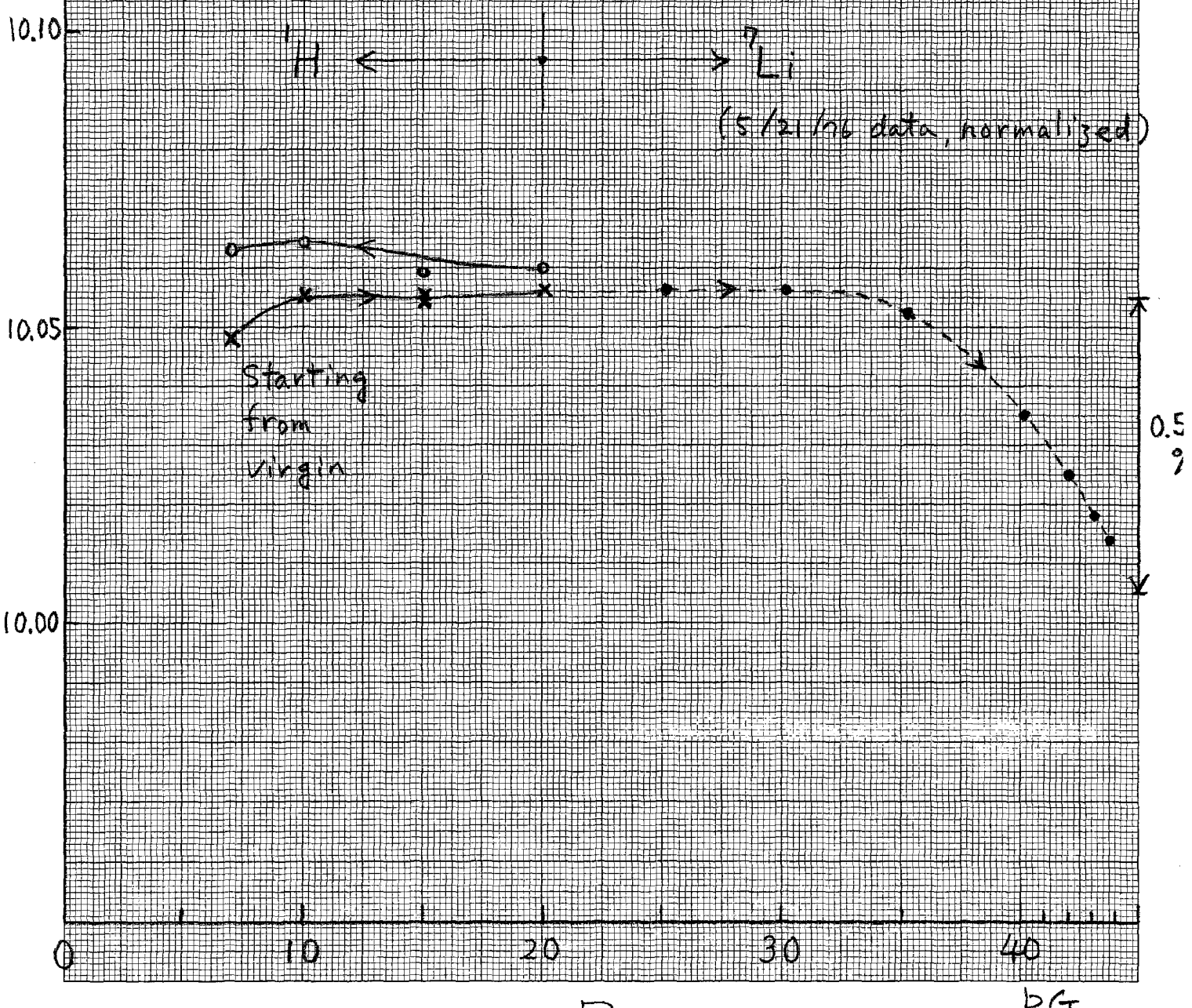

Fig. 9
Magnetization curves of E 5-1 with Core

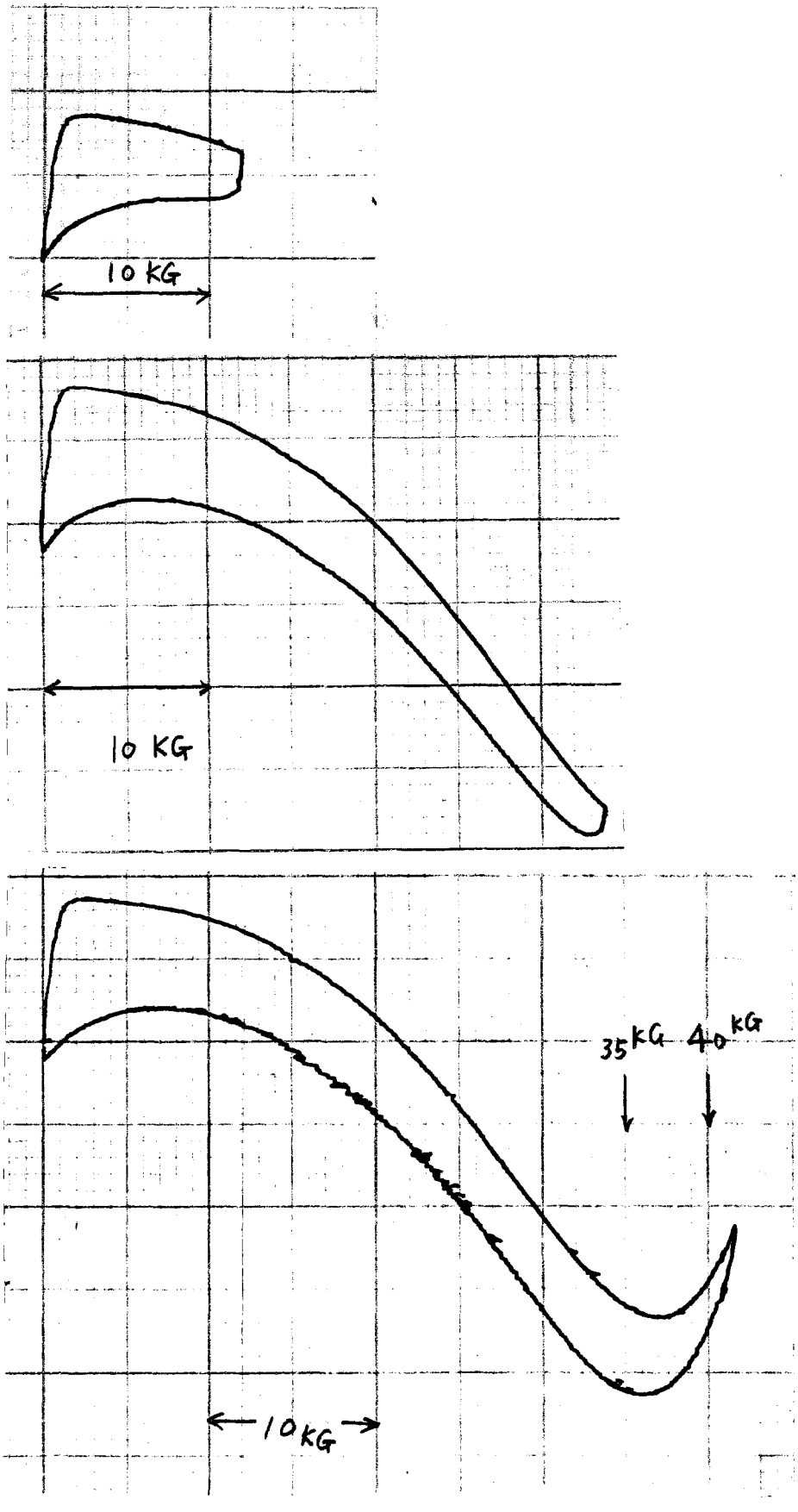

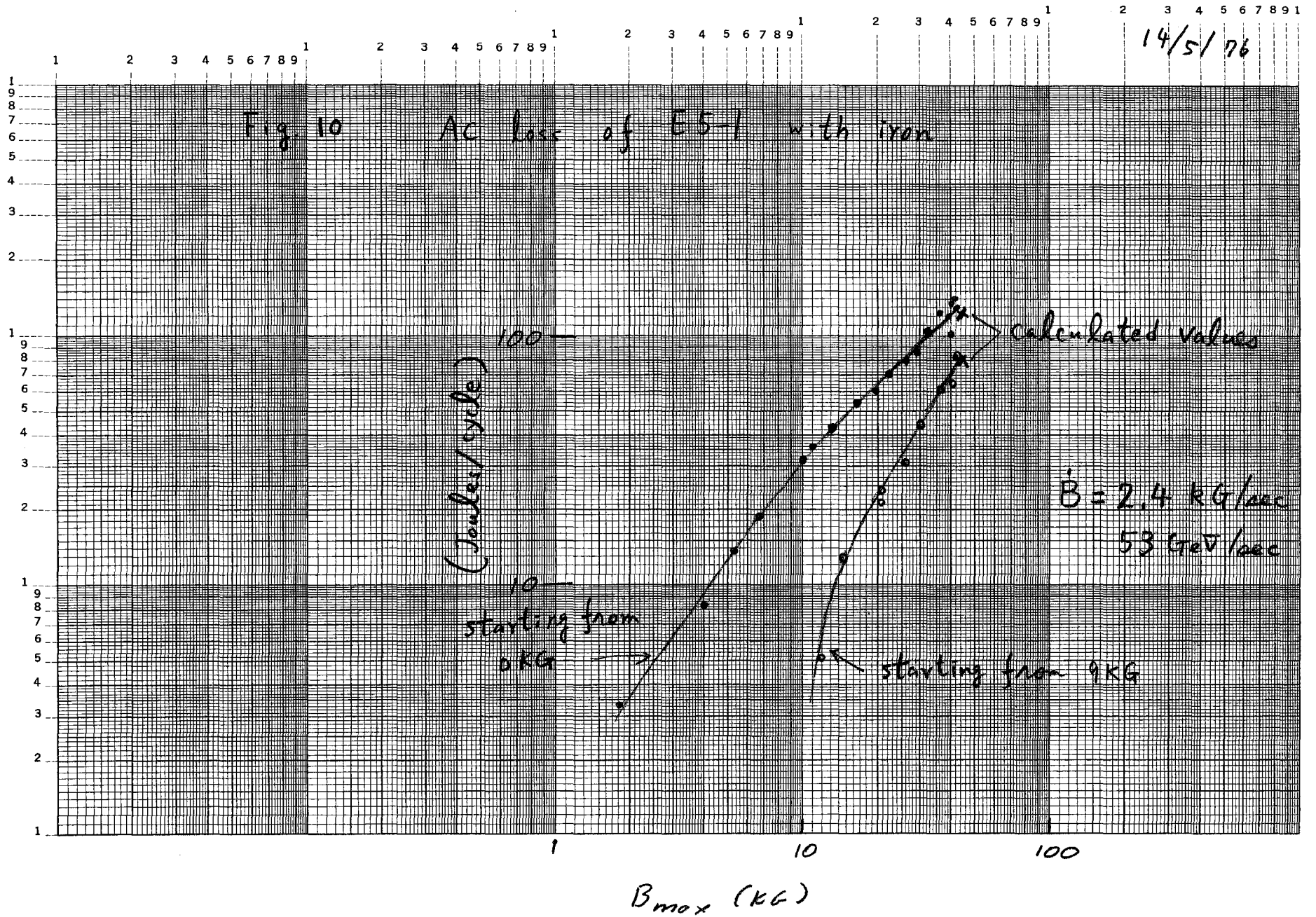
14/5/76
Fig. 10 AC loss of E5-1 with iron
Joule/cycle/kg
100
10
1
Calculated values
B = 2.4 kG/sec
53 GeV/sec
starting from 0 kG
starting from 9 kG
1
10
100
Bmax (KG)

Fig. 11 Longitudinal Field Shape at High Field 5/17/76

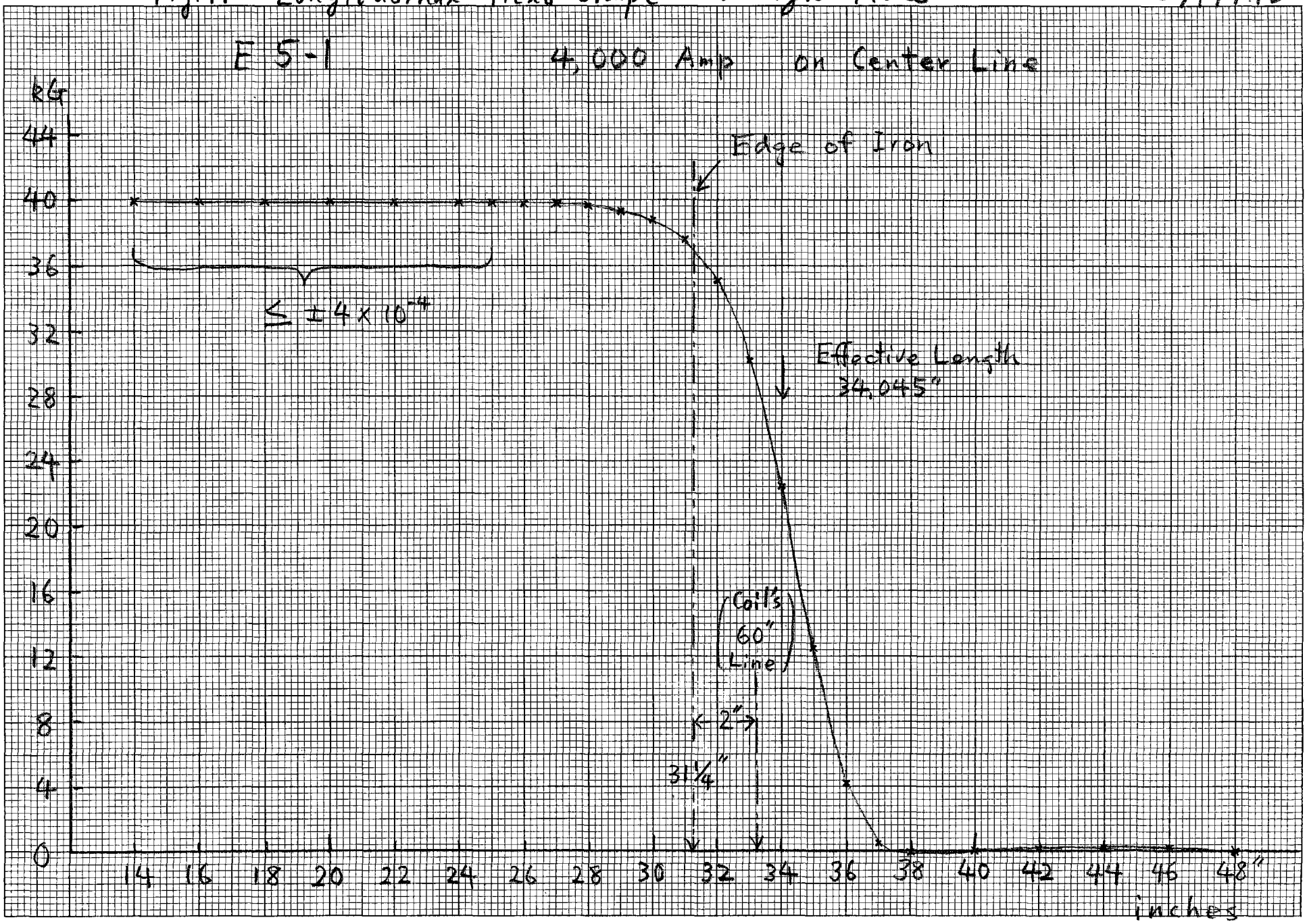

Fig. 12 Longitudinal Remanent Field 5/17/76

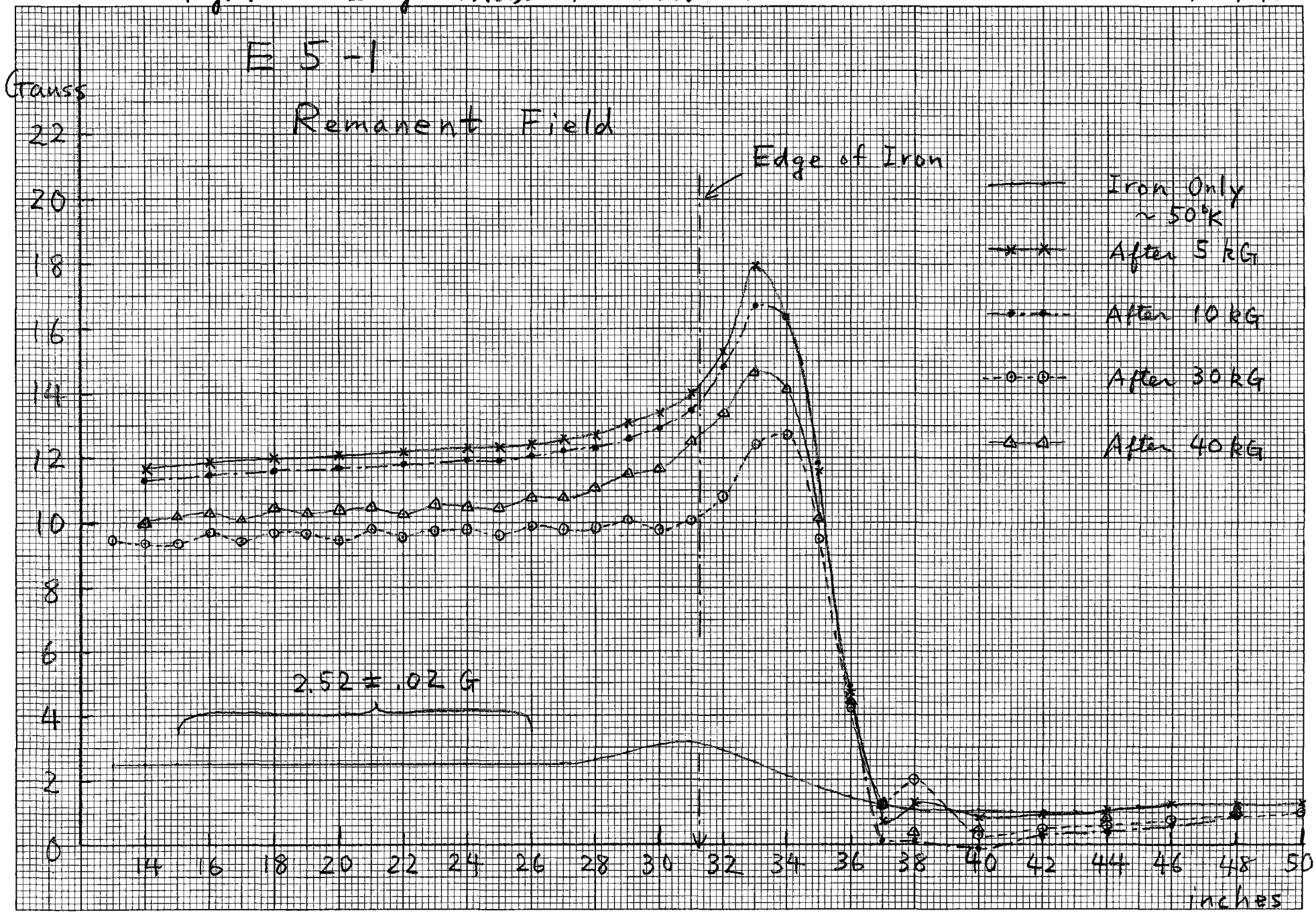

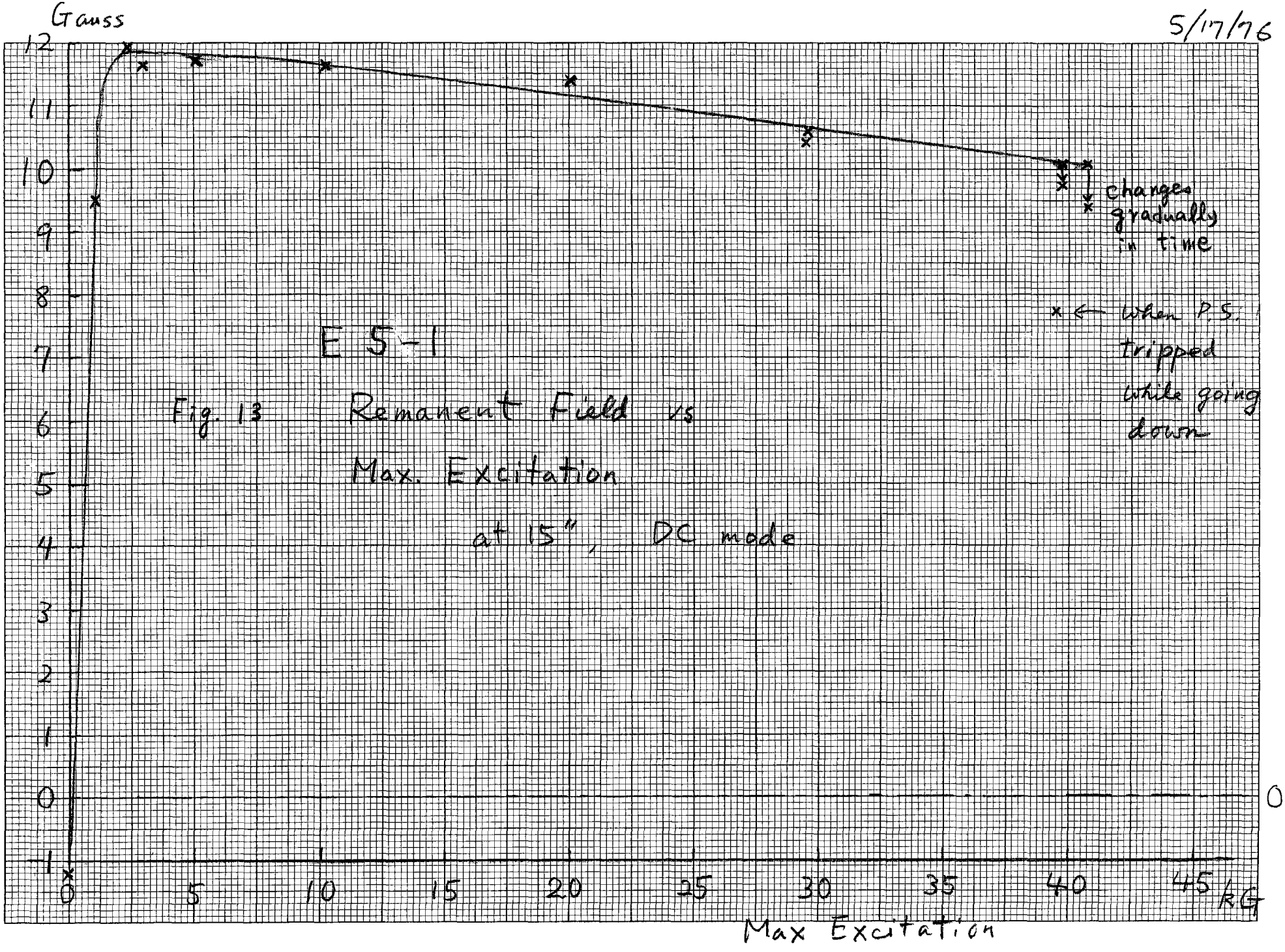
Gauss
5/17/76
12
11
10
9
8
7
6
5
4
3
2
1
0
1
0
5
10
15
20
25
30
35
40
45
KG
Max Excitation
changes gradually in time
× ← when P.S. tripped while going down
E S-1
Remanent Field vs
Max. Excitation
at 15", DC mode

Fig. 13

5/17/76

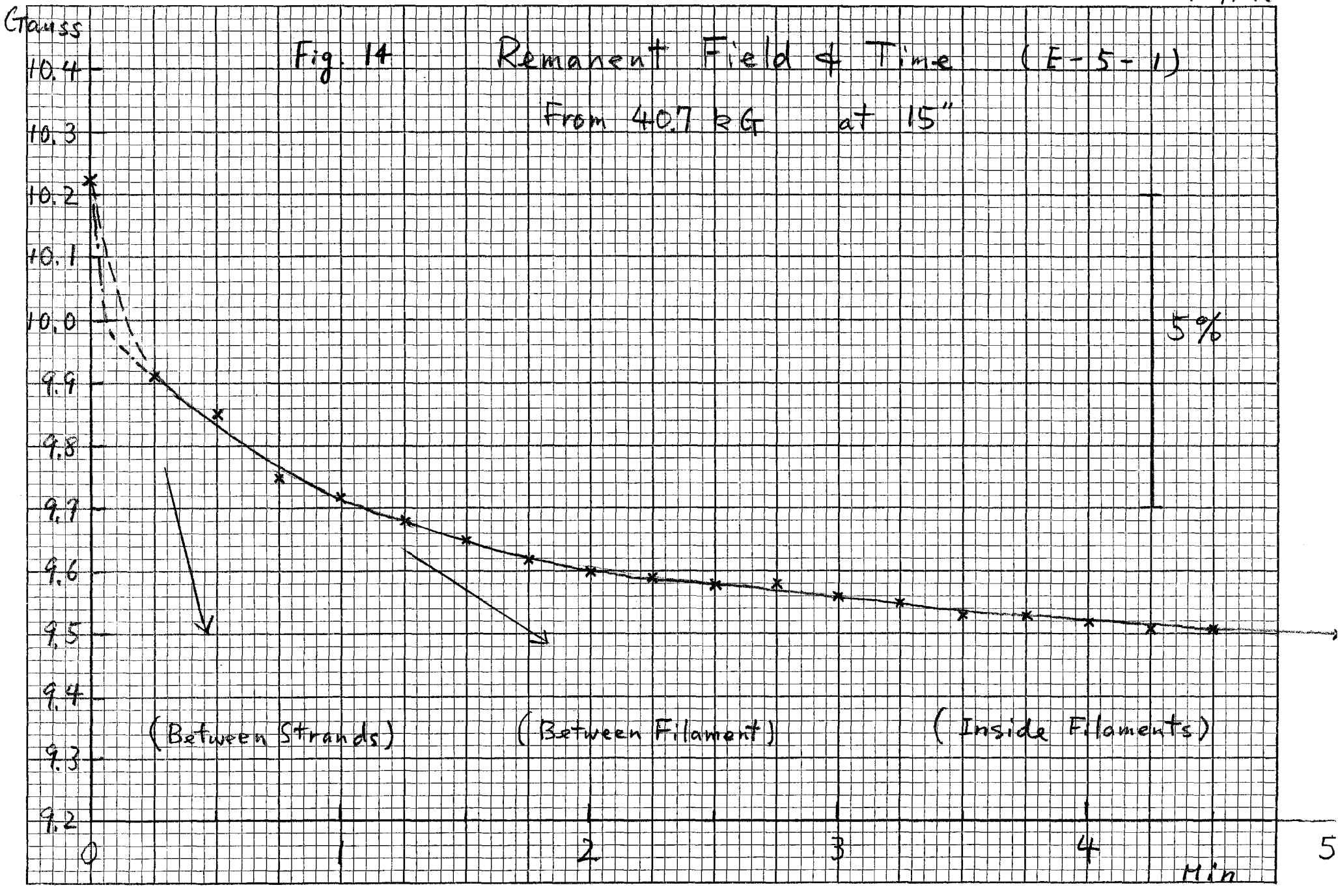


Fig. 14 Remanent Field & Time (E-5-1)

From 40.7 kG at 15"

E 5-1

Fig. 15 Remanent Field $B_y$
In Median Plane
at $Z = 15''$

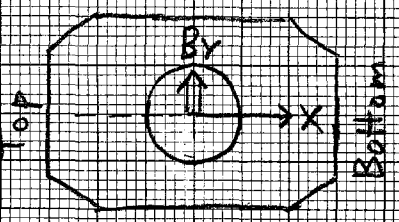


15

10

5

0

(Gauss)

after 10KG

after 20KG

Main Ring B2
Remanent
(at 1"
$\Delta B \doteq 0.2G$)

after 40 KG
(trip off)

E5-1 has
~ x20 higher
sextupole term
than M.R. B2

Some flux is still
trapped at bottom

at 50 ~ 60 K (normal state)

after quench

$-\frac{1}{2}''$ $-\frac{1}{4}''$ 0 $\frac{1}{4}''$ $\frac{1}{2}''$ x

E 5-1

Fig. 16 Remanent Field $B_y$ In Vertical Plane at $Z = 15''$

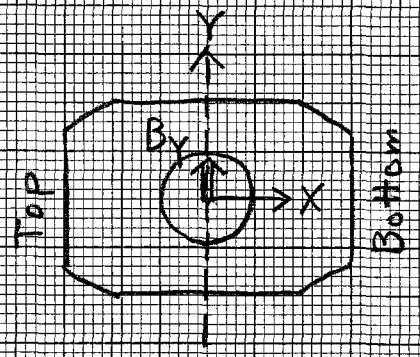


15

10

5

0

(Gauss)

after 10 kG

after 20 kG

after 40 kG (trip off)

at 50~60k (normal state)

after quench

$-\frac{1}{2}''$ $-\frac{1}{4}''$ 0 $\frac{1}{4}''$ $\frac{1}{2}''$ y

5/17/76

Fig. 17 Field shape at ~ 40KG

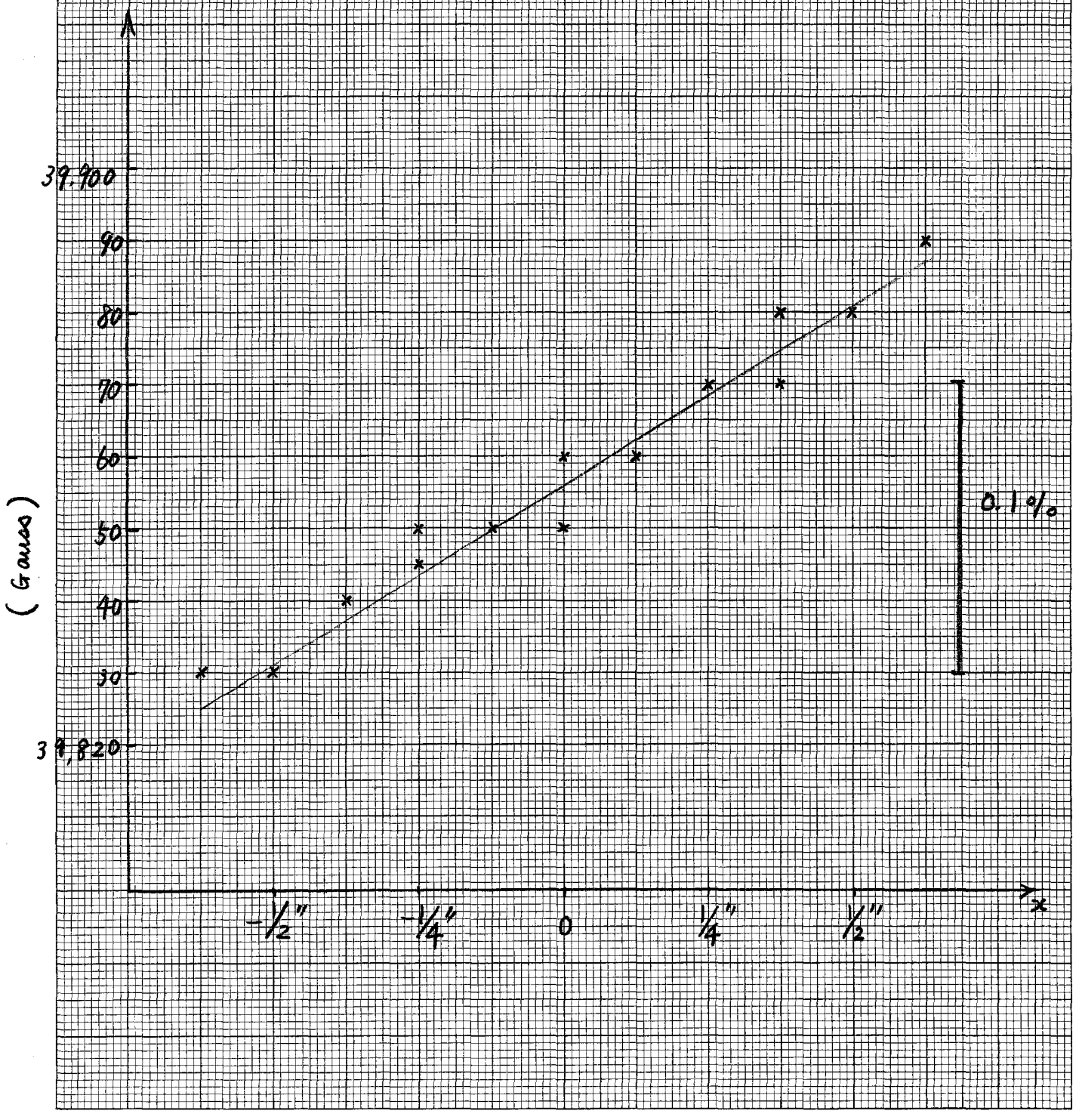

5/27/76

Fig. 18 Remanent Field

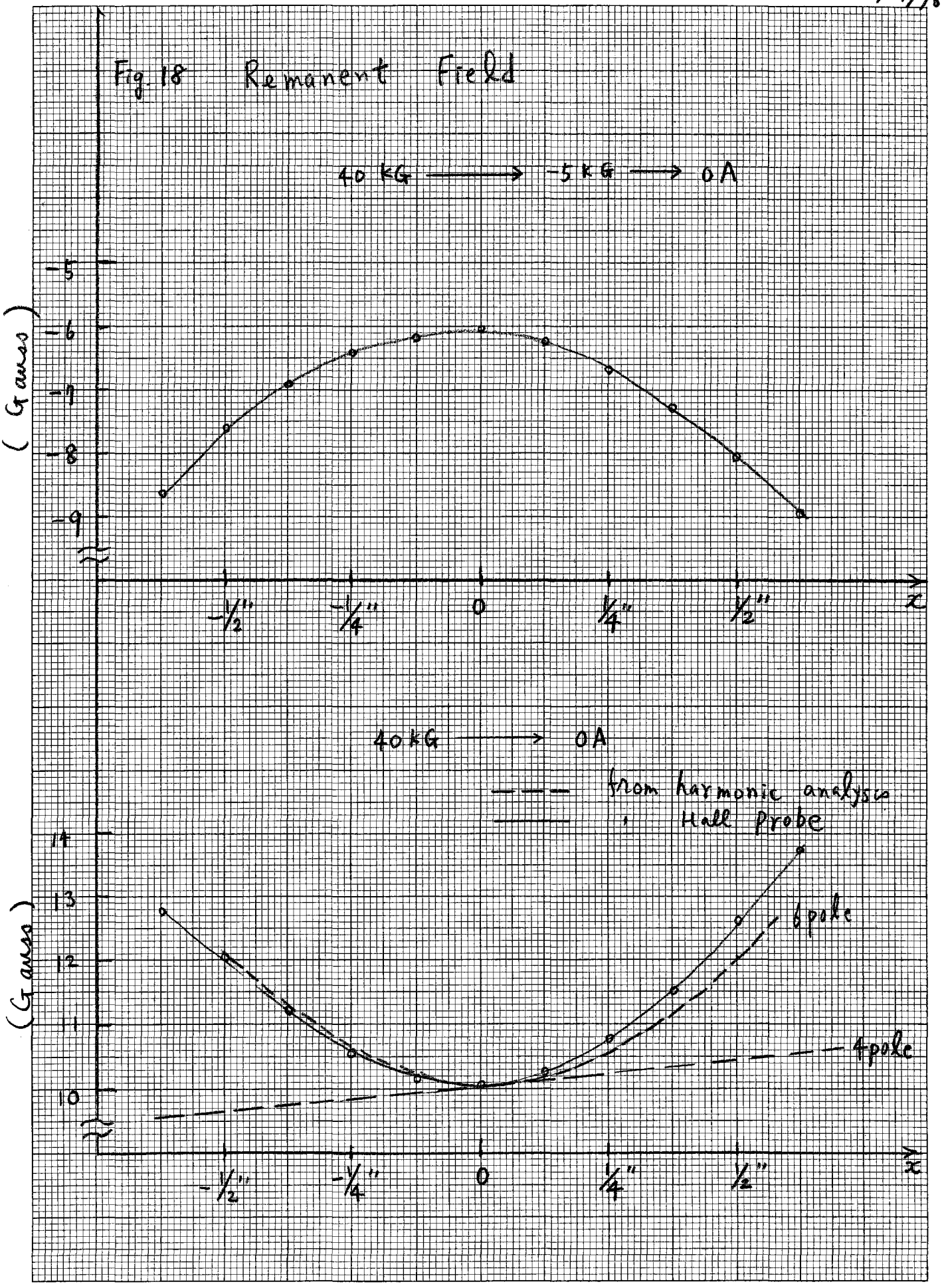

5/27/76

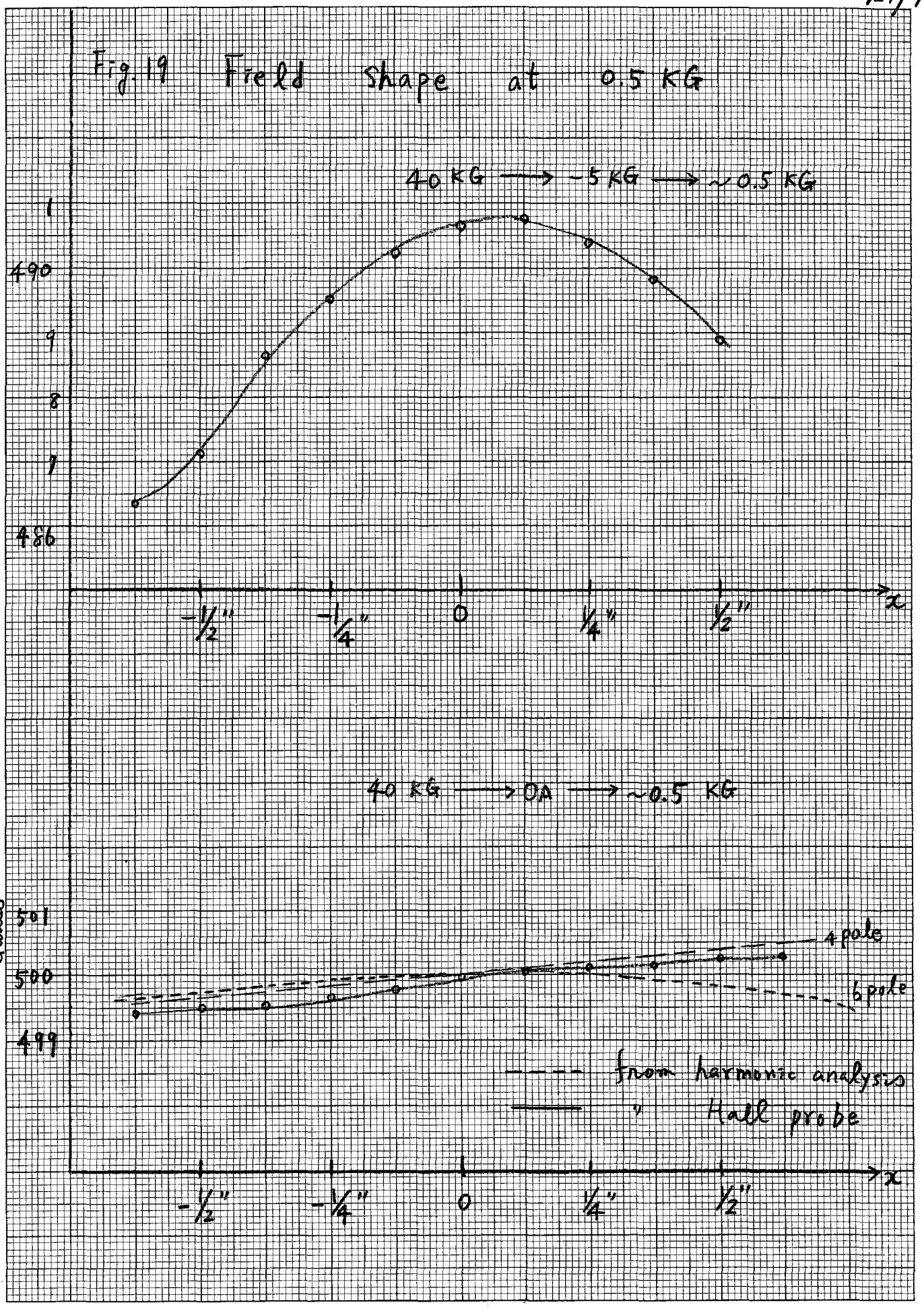

5/27/76

Fig. 20 Field shape at ~ 1 KG

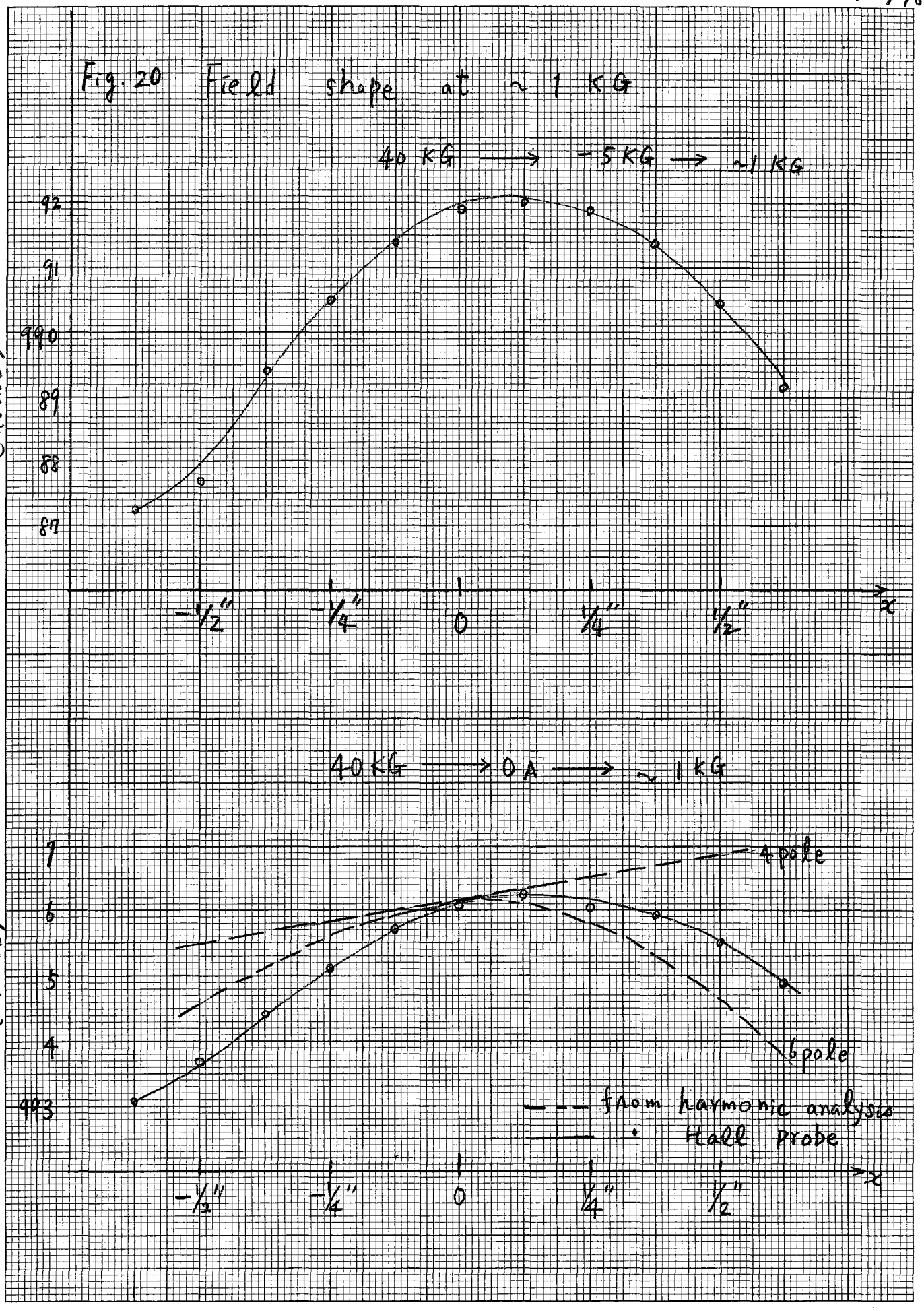

5/18/76

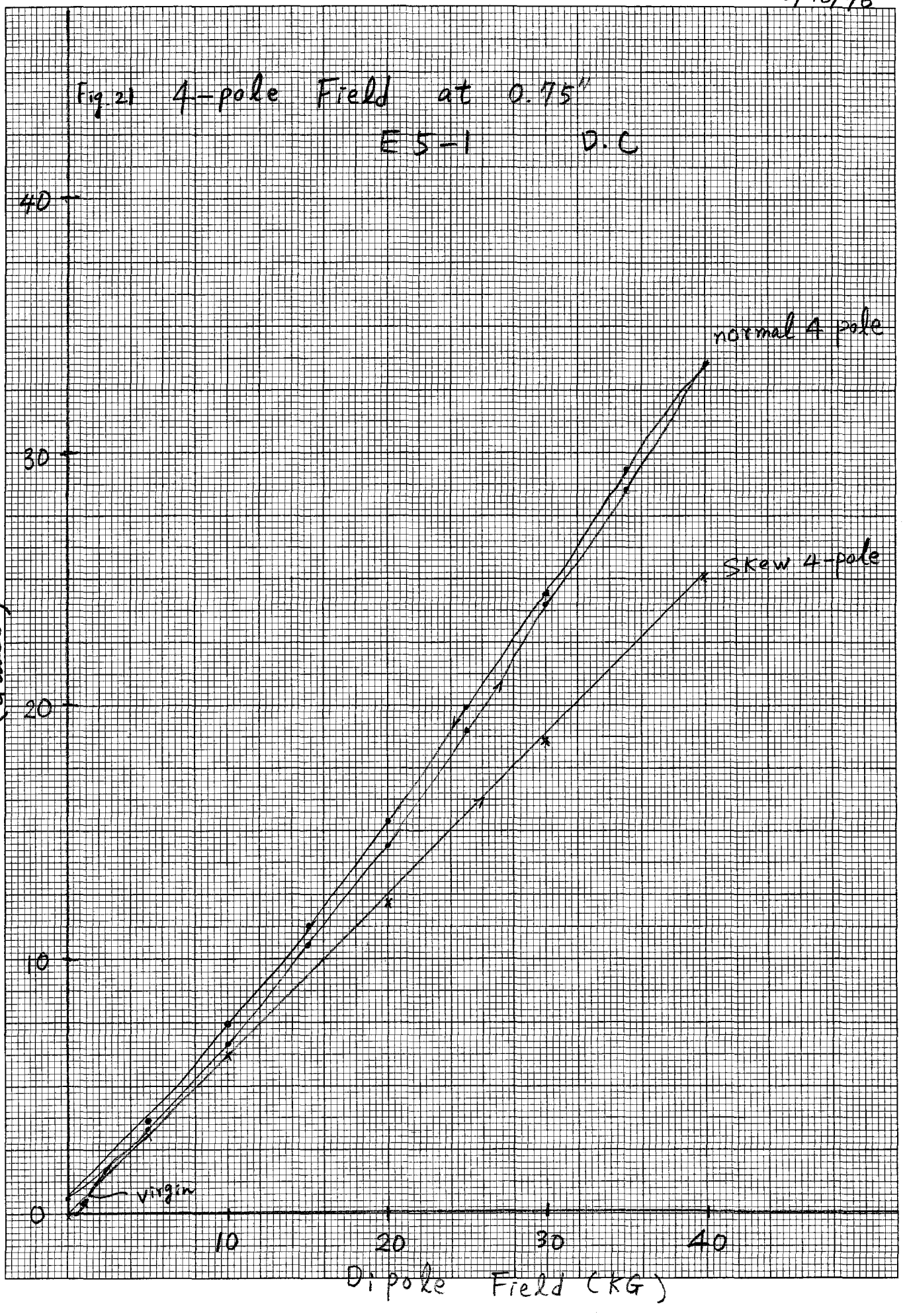

5/18/76

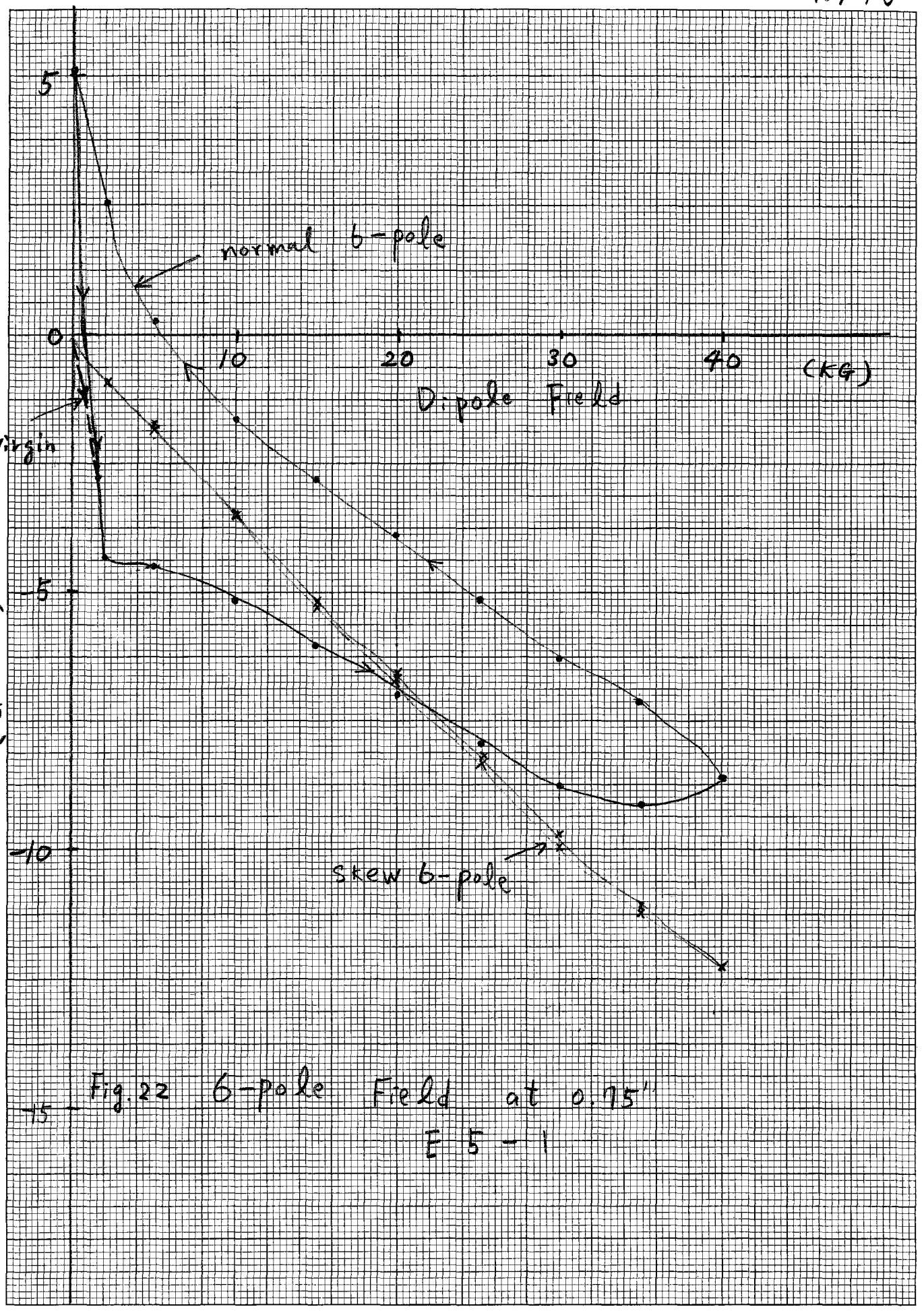


Fig. 22 6-Pole Field at 0.75"

E 5 - 1

5/18/76

Fig. 23 8, 10-pole field at 0.75"

E 5-1 D.C

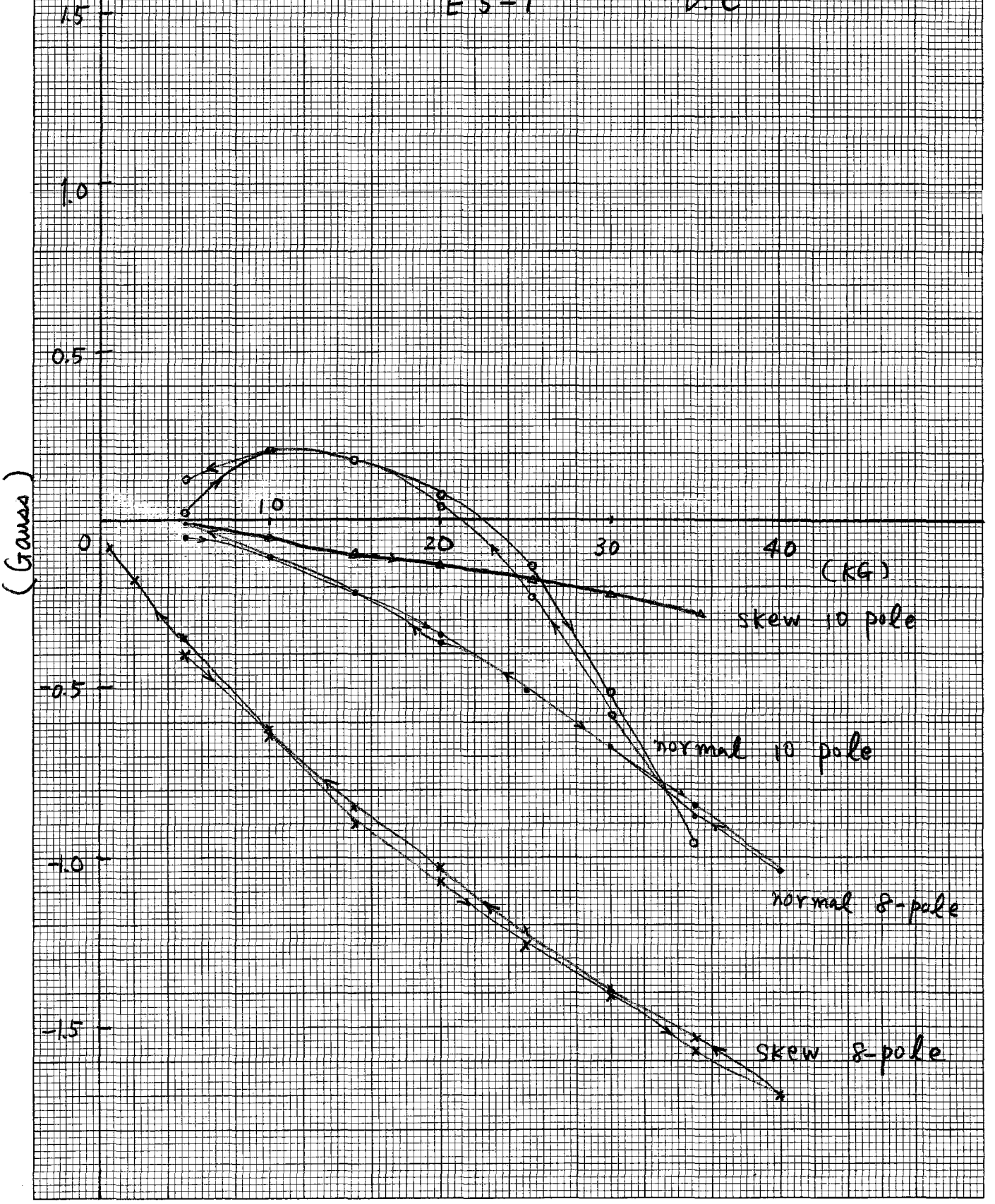

Fig. 24 4-pole coefficient at mid plane

E 5-1

$$B_y(y=0) = B_0(1 + b_1 x + b_2 x^2 + \cdots)$$

$$B_x(y=0) = B_0(a_1 x + a_2 x^2 + \cdots)$$

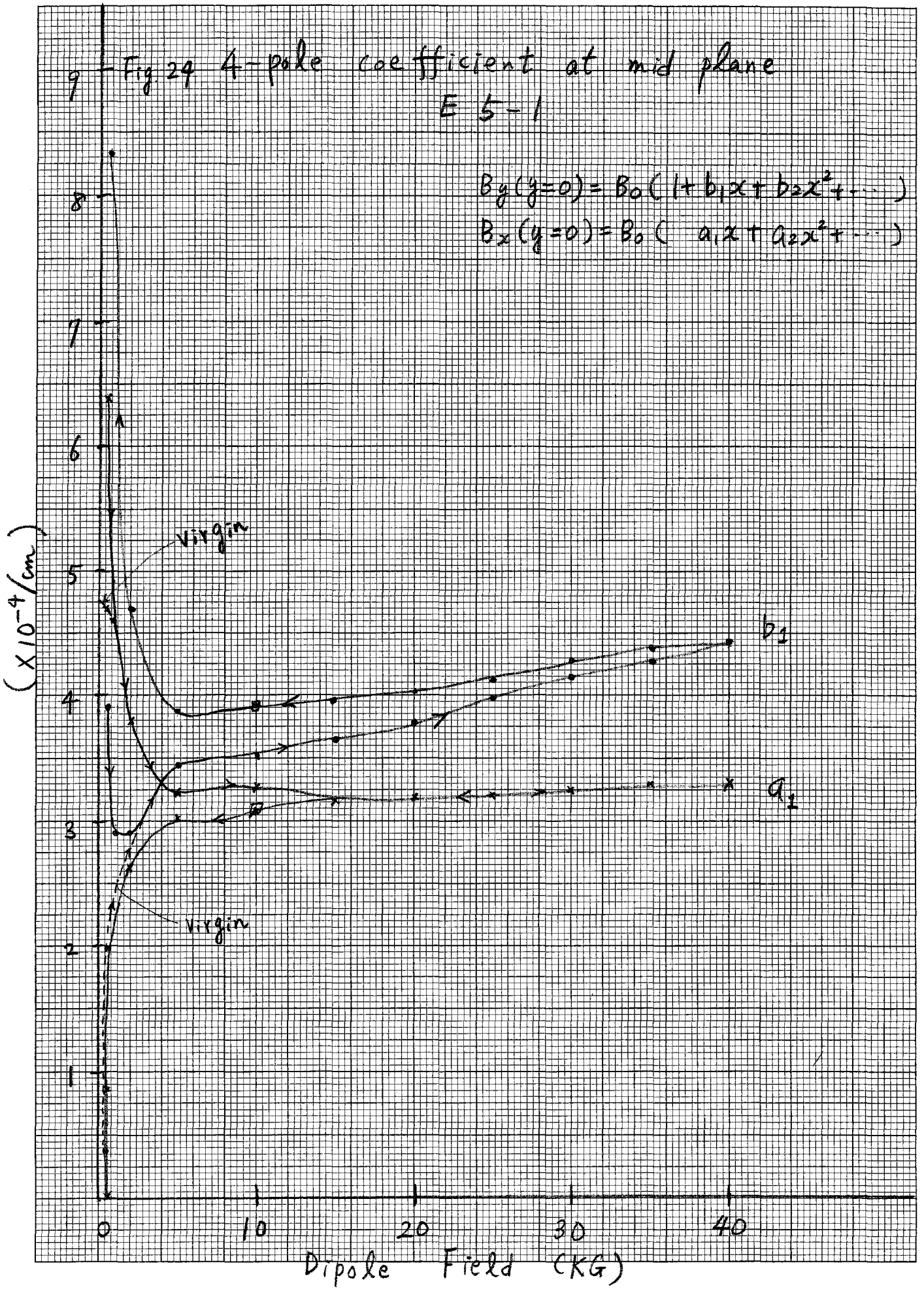

Fig. 25 6 pole coefficient in mid plane

E-5-1

$$\begin{cases} B_y\,(y=0) = B_0(1 + b_1x + b_2x^2 + \cdots) \\ B_x\,(y=0) = B_0(a_1x + a_2x^2 + \cdots) \end{cases}$$

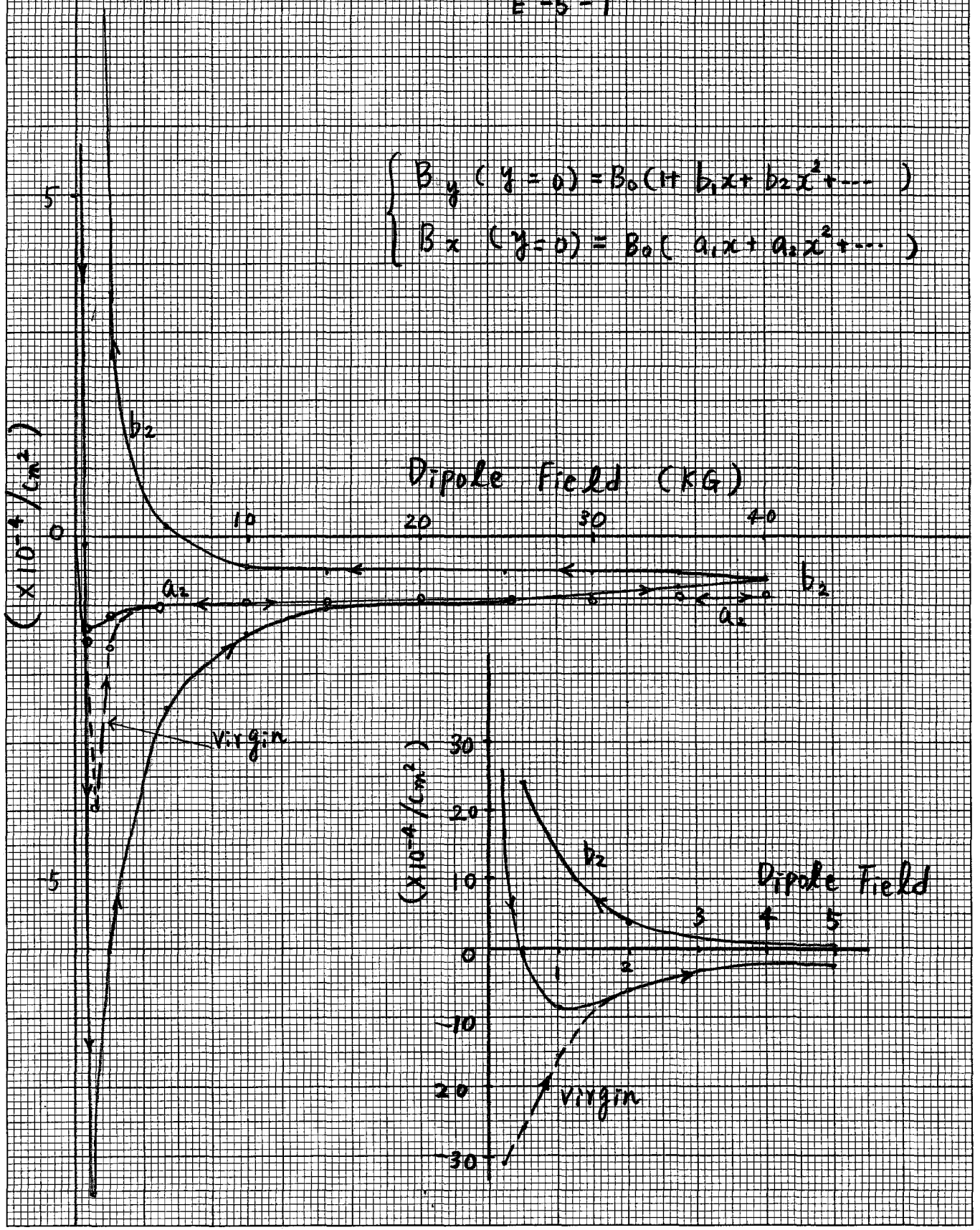

E-5-1

Fig 26 Variation of $\frac{8}{10}$ pole coefficient

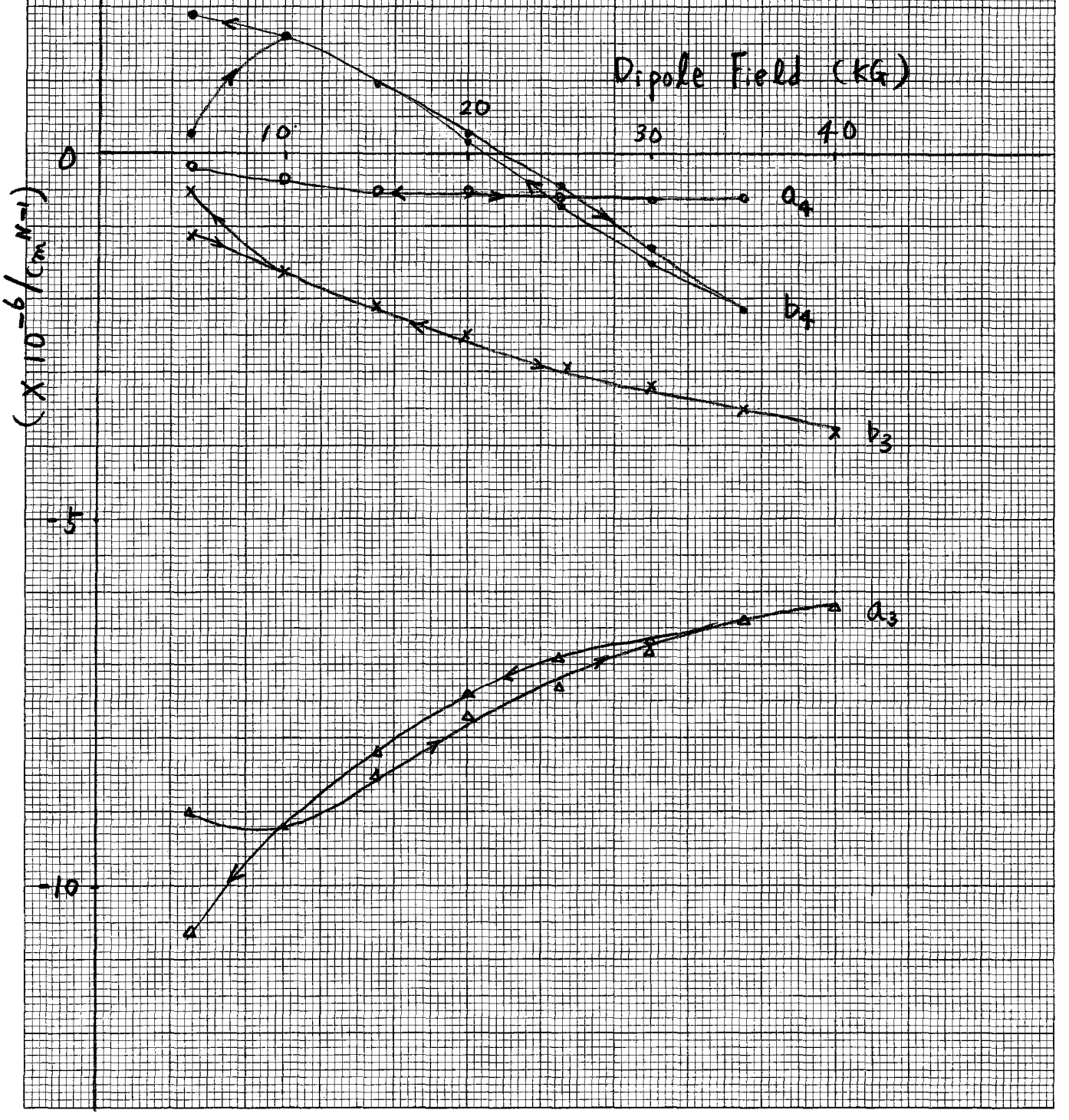

5/19/76

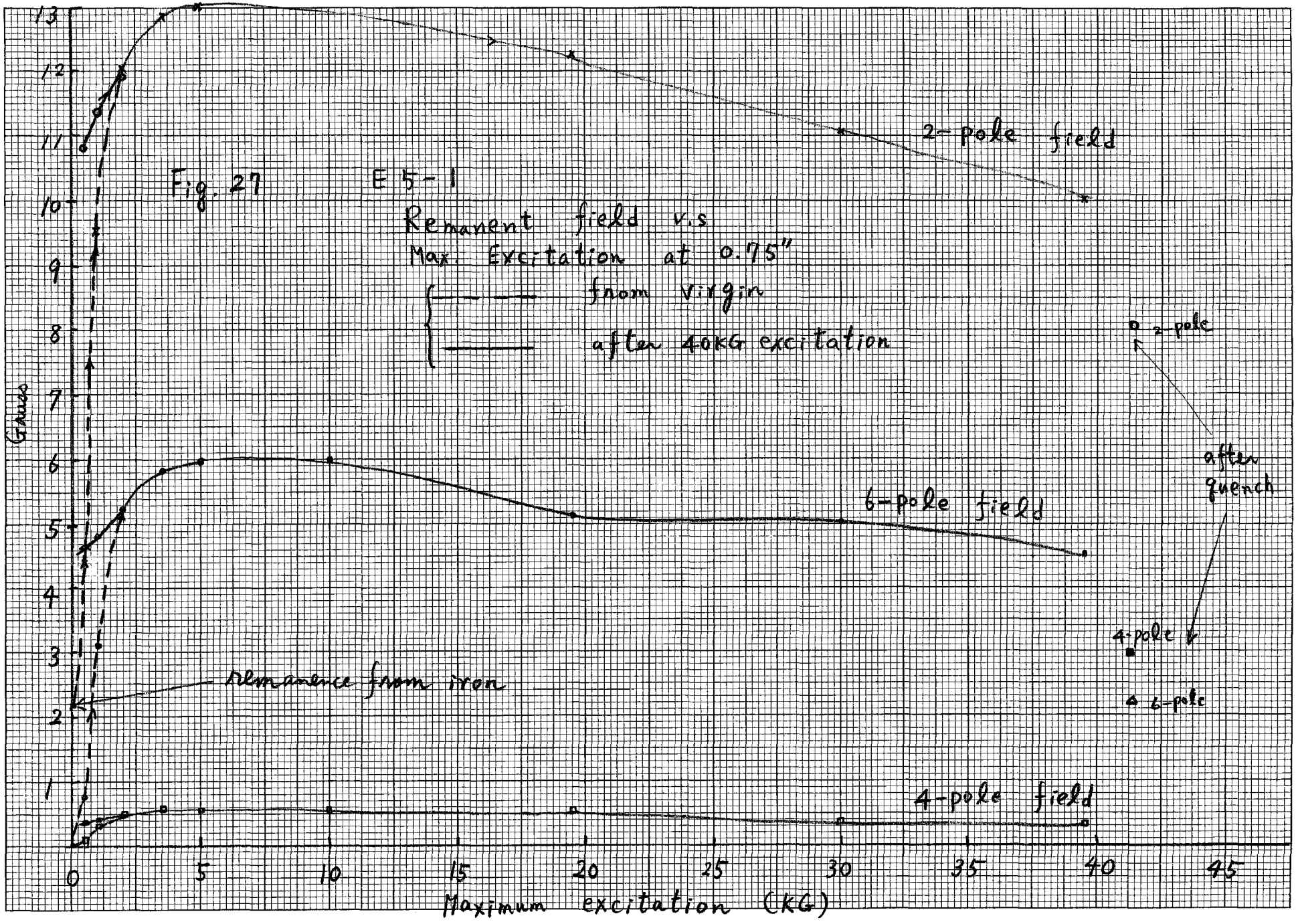
Fig. 27
E 5-1
Remanent field v.s
Max. Excitation at 0.75"
from virgin
after 40kG excitation
2-pole field
6-pole field
4-pole field
remanence from iron
2-pole
after quench
4-pole
6-pole
Gauss
Maximum excitation (kG)
0
5
10
15
20
25
30
35
40
45
1
2
3
4
5
6
7
8
9
10
11
12
13

E 5 – 1

Fig. 28 4-pole Coef. of Remanent Field v.s Maximum Excitation Field

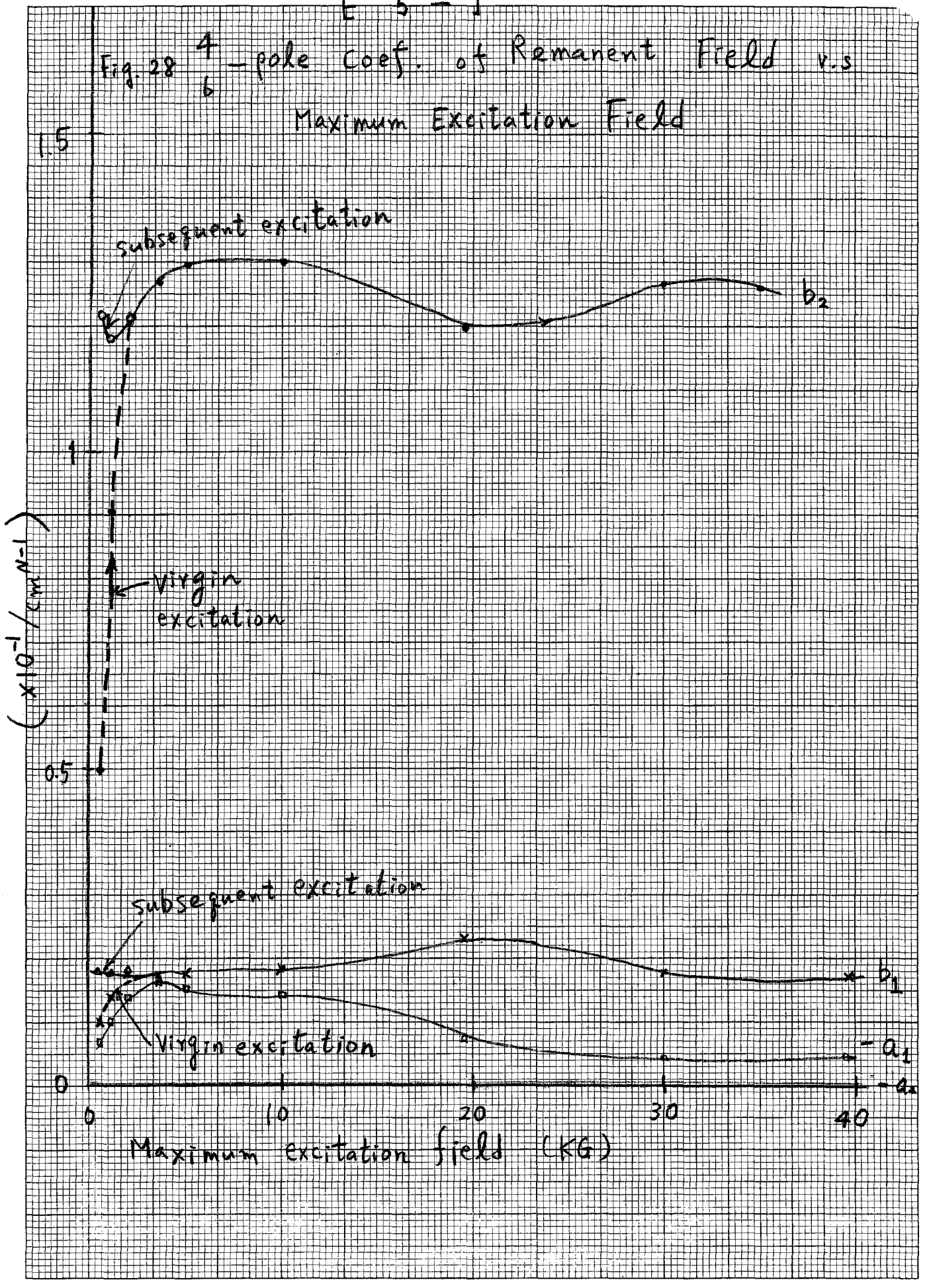

Fig. 29

AC H Pole Field at .75"

E 5-1 ($\dot{B}$ = 2.2 KG/sec)

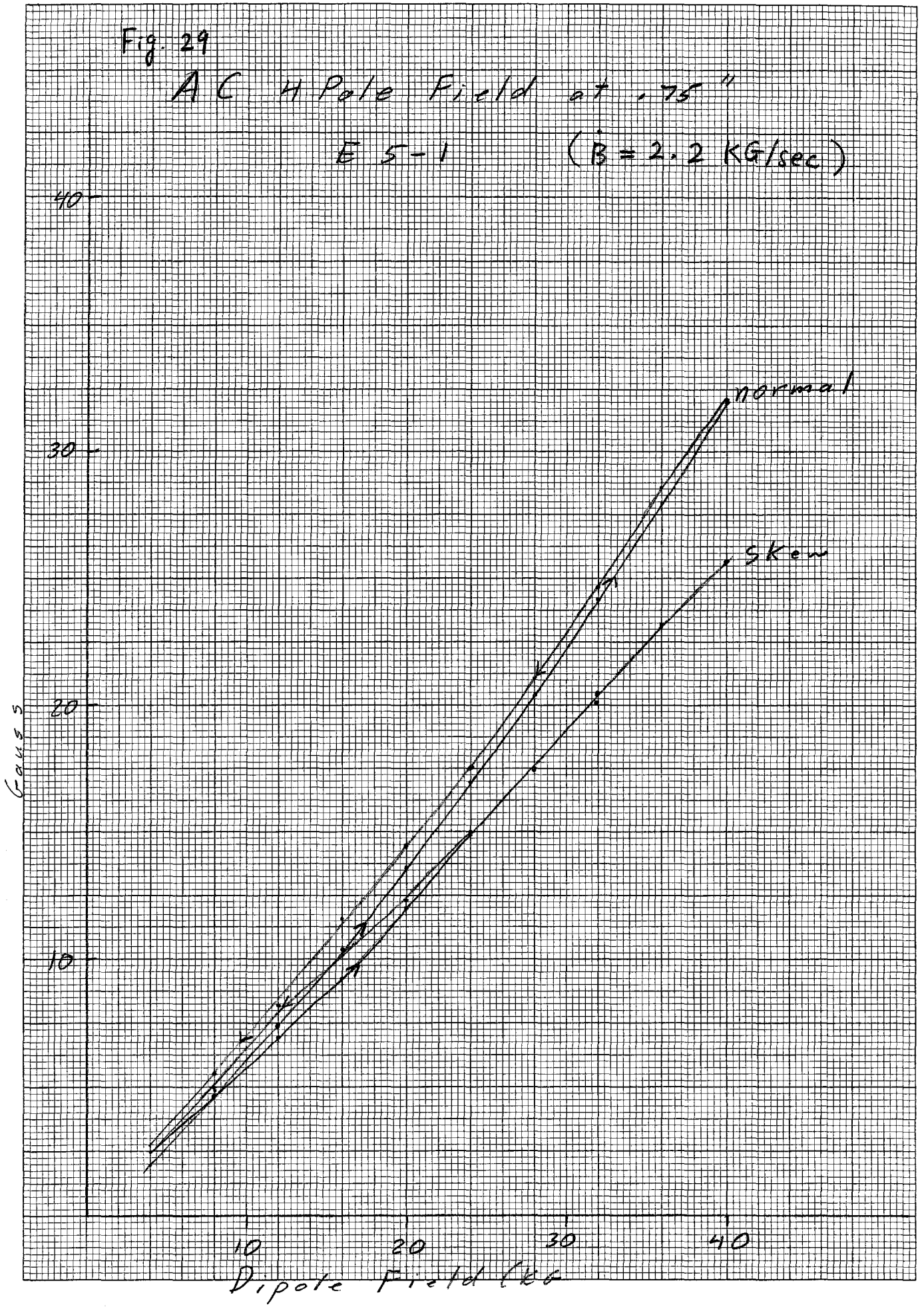

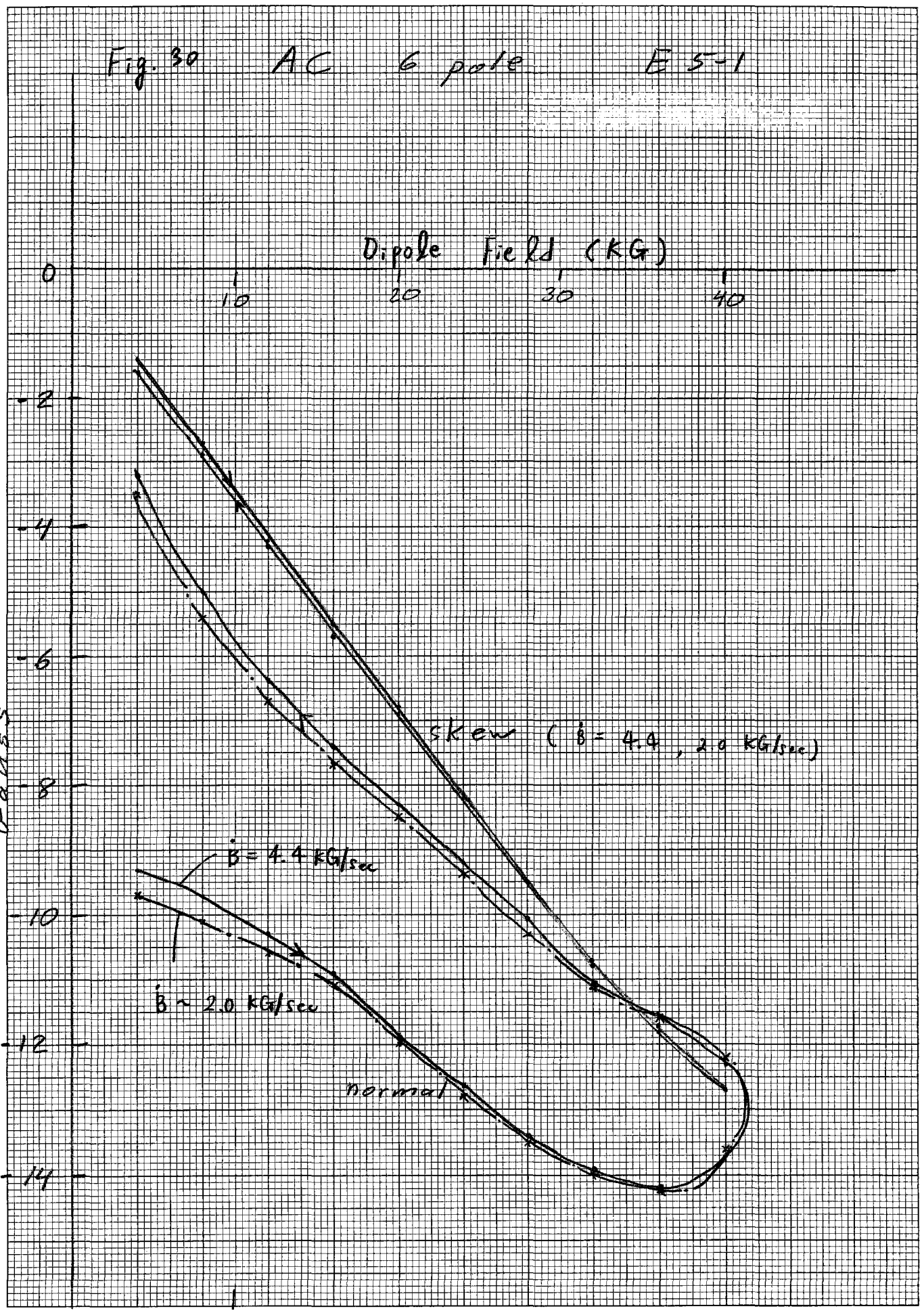
Fig. 30 AC 6 pole E 5-1
Dipole Field (KG)
0
10
20
30
40
-2
-4
-6
-8
-10
-12
-14
(Gauss)
skew ( Ḃ = 4.4 , 2.0 kG/sec)
Ḃ = 4.4 kG/sec
Ḃ = 2.0 kG/sec
normal

Fig. 31 AC 4 pole E 5-1

coefficients at mid plane

($\dot{B}$ = 2.2 KG/sec)

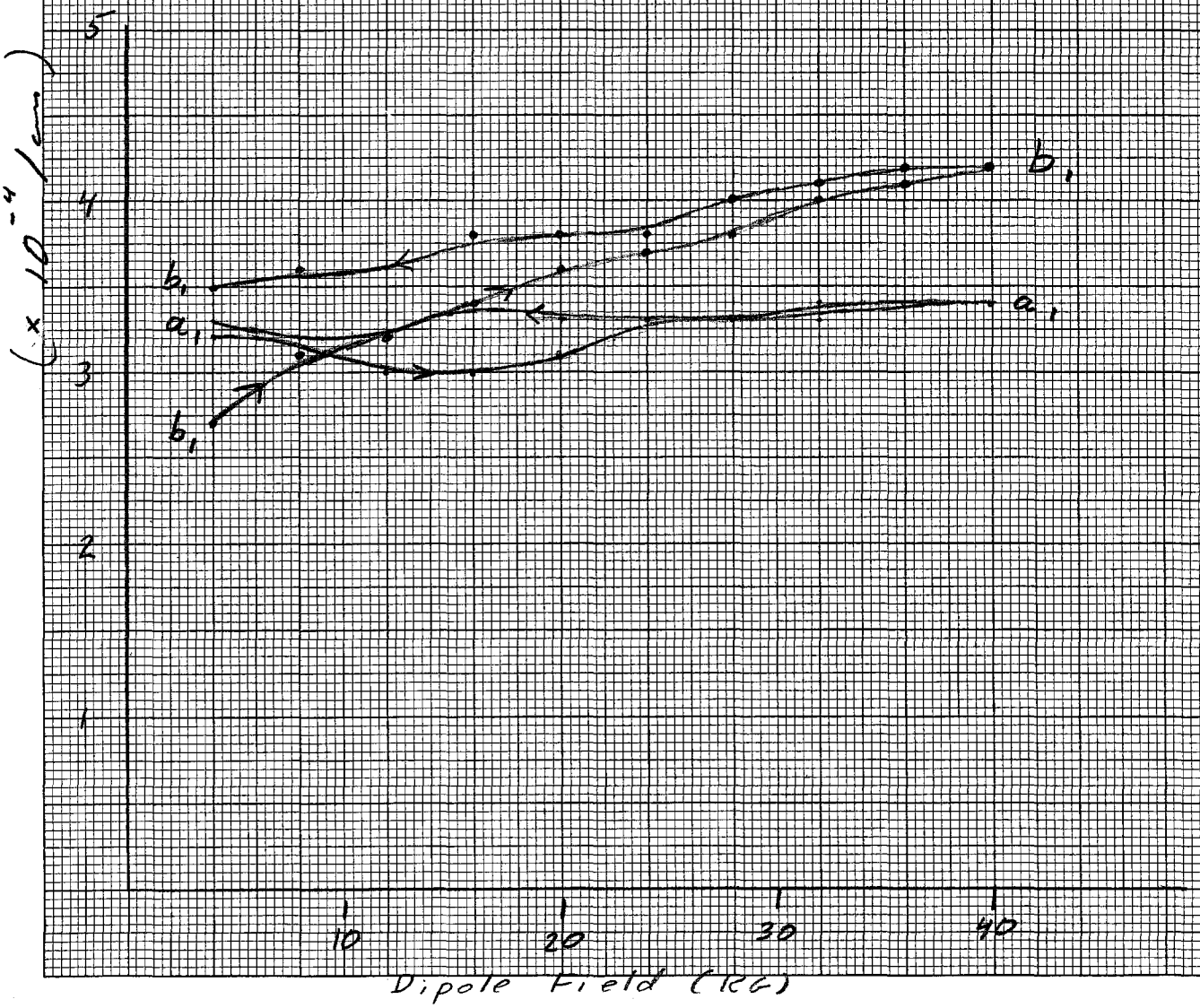

Fig. 32 AC 6-pole coefficients at mid plane

E 5-1 ($\dot{B}$ = 4.4 KG/sec)

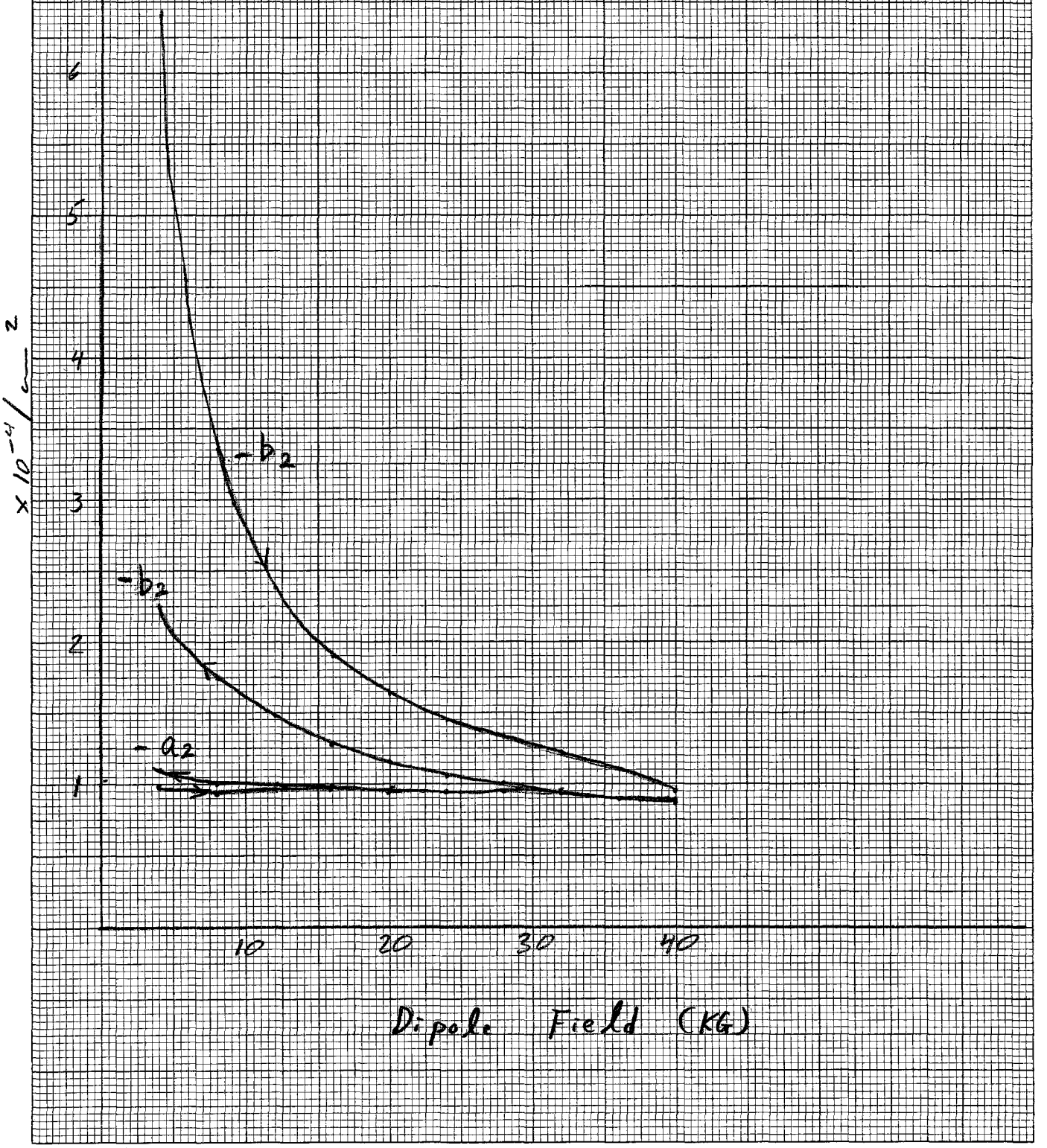

5/20/76

Fig. 33 4-pole Field in the end region (1' long)

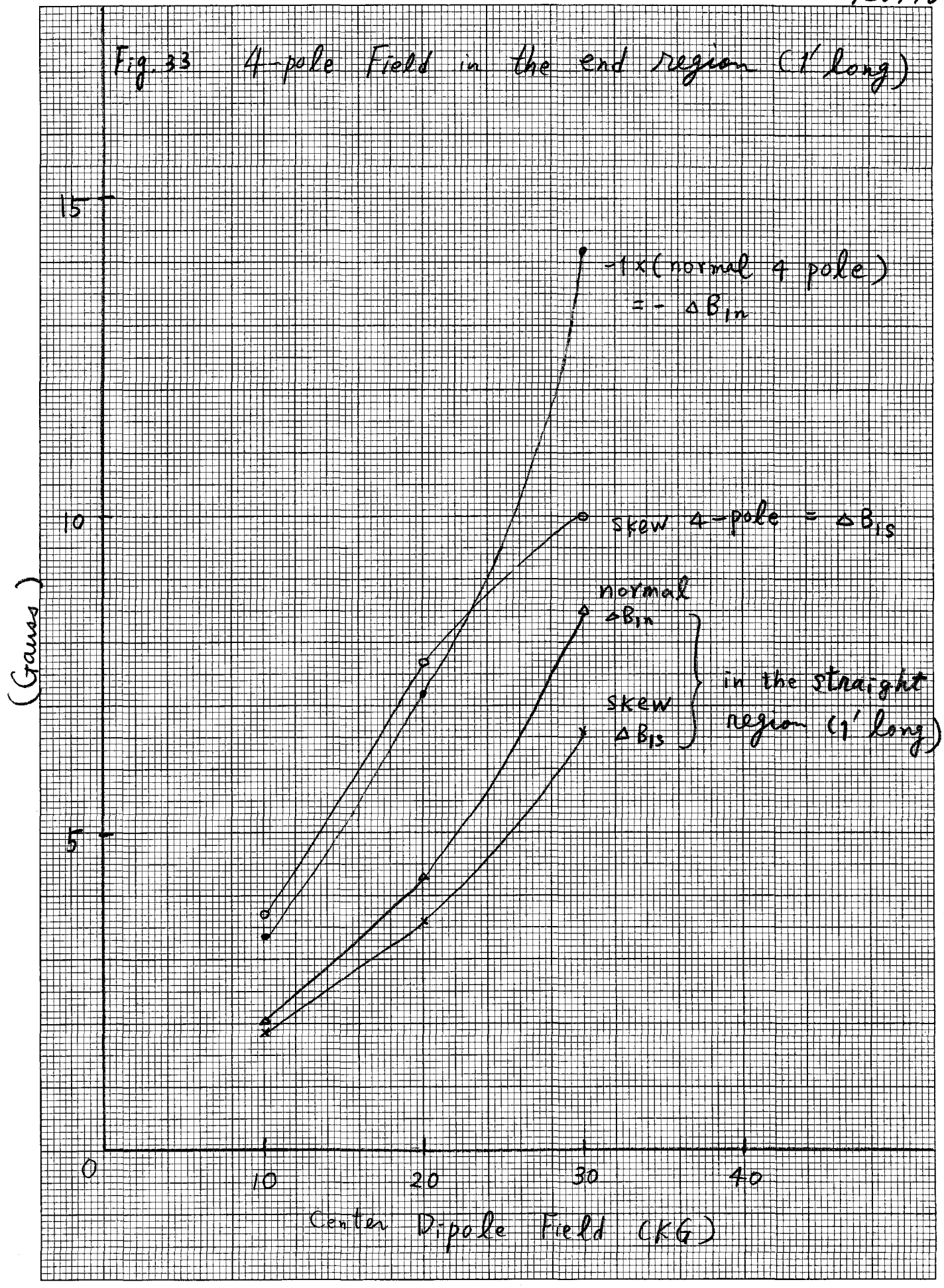

5/20/76

Fig 34 normal 6-pole field in the end region (1' long)
($\Delta B_2$)